THE UNIVERSITY OF MICHIGAN RESEARCH INSTITUTE
ANN ARBOR

INVESTIGATION OF MICROWAVE PROPERTIES OF FERROELECTRIC MATERIALS

FINAL REPORT

Period Covering February 1, 1958 to January 31, 1959

Electronic Defense Group
Department of Electrical Engineering

Prepared by:

C. B. Sharpe, Principal Investigator
C. G. Brockus

Approved by: 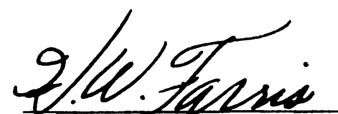
H. W. Farris

Project 2732

Contract No. DA-36-039 sc-75003
Department of the Army
Signal Corps

March 1959

TABLE OF CONTENTS

LIST OF ILLUSTRATIONS iii

ACKNOWLEDGEMENT vi

ABSTRACT vii

FOREWORD 1

1. INTRODUCTION 3

2. METHOD 6

2.1 General 6
2.2 Theory 7
2.3 Experimental Equipment and Procedure 13

3. DISCUSSION OF RESULTS 17

4. CONCLUSIONS 20

REFERENCES 60

DISTRIBUTION LIST 61

LIST OF ILLUSTRATIONS

Figure 1	Sample and Sample Holder	8
Figure 2	Equivalent Circuit for Sample Holder	10
Figure 3	Sample Holder Assembly	14
Figure 4	Experimental Arrangement for the Measurement of the Complex Dielectric-Constant of Ferroelectrics	16
Figure 5	Relative Dielectric Constant vs. Temperature for $BaTiO_3$	22
Figure 6	Relative Dielectric Constant vs. Temperature for Hot-Pressed $BaTiO_3$ (PT)	23
Figure 7	Relative Dielectric Constant vs. Temperature for 99.95% $BaTiO_3$: 0.05% Fe_2O_3	24
Figure 8	Relative Dielectric Constant vs. Temperature for 35% $PbTiO_3$: 65% $SrTiO_3$	25
Figure 9	Relative Dielectric Constant vs. Temperature for 75% $BaTiO_3$: 25% $SrTiO_3$	26
Figure 10	Relative Dielectric Constant vs. Temperature for 72% $BaTiO_3$: 27% $SrTiO_3$: 1% Fe_2O_3	27
Figure 11	Relative Dielectric Constant vs. Temperature for 60% $BaTiO_3$: 40% $SrTiO_3$	28
Figure 12	Relative Dielectric Constant vs. Frequency for $BaTiO_3$	30
Figure 13	Relative Dielectric Constant vs. Bias Field for $BaTiO_3$	31
Figure 14	Relative Dielectric Constant vs. Frequency for Hot-Pressed $BaTiO_3$ (PT)	32
Figure 15	Relative Dielectric Constant vs. Bias Field for Hot-Pressed $BaTiO_3$ (PT)	33
Figure 16	Relative Dielectric Constant vs. Frequency for 99.95% $BaTiO_3$: 0.05% Fe_2O_3	34
Figure 17	Relative Dielectric Constant vs. Bias Field for 99.95% $BaTiO_3$: 0.05% Fe_2O_3	35

Figure 18 Relative Dielectric Constant vs. Frequency for 75% $BaTiO_3$: 25% $SrTiO_3$ 36

Figure 19 Relative Dielectric Constant vs. Bias Field for 75% $BaTiO_3$: 25% $SrTiO_3$ 37

Figure 20 Relative Dielectric Constant vs. Frequency for 74% $BaTiO_3$: 25% $SrTiO_3$: 1% Fe_2O_3 38

Figure 21 Relative Dielectric Constant vs. Frequency for 74% $BaTiO_3$: 25% $SrTiO_3$: 1% Fe_2O_3 39

Figure 22 Relative Dielectric Constant vs. Frequency for 73% $BaTiO_3$: 25% $SrTiO_3$: 2% Mn 40

Figure 23 Relative Dielectric Constant vs. Bias Field for 73% $BaTiO_3$: 25% $SrTiO_3$: 2% Mn 41

Figure 24 Relative Dielectric Constant vs. Frequency for 73% $BaTiO_3$: 25% $SrTiO_3$: 2% Ni 42

Figure 25 Relative Dielectric Constant vs. Bias Field for 73% $BaTiO_3$: 25% $SrTiO_3$: 2% Ni 43

Figure 26 Relative Dielectric Constant vs. Frequency for 72% $BaTiO_3$: 27% $SrTiO_3$: 1% Fe_2O_3 44

Figure 27 Relative Dielectric Constant vs. Bias Field for 72% $BaTiO_3$: 27% $SrTiO_3$: 1% Fe_2O_3 45

Figure 28 Relative Dielectric Constant vs. Frequency for 69% $BaTiO_3$: 30% $SrTiO_3$: 1% Fe_2O_3 46

Figure 29 Relative Dielectric Constant vs. Bias Field for 69% $BaTiO_3$: 30% $SrTiO_3$: 1% Fe_2O_3 47

Figure 30 Relative Dielectric Constant vs. Frequency for 60% $BaTiO_3$: 40% $SrTiO_3$ 48

Figure 31 Relative Dielectric Constant vs. Bias Field for 60% $BaTiO_3$: 40% $SrTiO_3$ 49

Figure 32 Relative Dielectric Constant vs. Frequency for 96% $BaTiO_3$: 4% $PbTiO_3$ 50

Figure 33 Relative Dielectric Constant vs. Bias Field for 96% $BaTiO_3$: 4% $PbTiO_3$ 51

Figure 34 Relative Dielectric Constant vs. Frequency for $PbTiO_3$ 52

Figure 35 Relative Dielectric Constant vs. Bias Field for $PbTiO_3$ 53

Figure 36 Relative Dielectric Constant vs. Frequency for 35% $PbTiO_3$: 65% $SrTiO_3$ 54

Figure 37 Relative Dielectric Constant vs. Bias Field for 35% $PbTiO_3$: 65% $SrTiO_3$ 55

Figure 38 Relative Dielectric Constant vs. Frequency for Hot-Pressed $Cd_2Nb_2O_7$ 56

Figure 39 Relative Dielectric Constant vs. Bias Field for Hot-Pressed $Cd_2Nb_2O_7$ 57

Figure 40 Relative Dielectric Constant vs. Frequency for Hi-Q-91 58

Figure 41 Relative Dielectric Constant vs. Bias Field for Hi-Q-91 59

ACKNOWLEDGEMENT

The authors are indebted to H. Diamond for his advice and assistance in the early phases of the work and for his aid in selecting the ferroelectrics which were investigated. A special acknowledgement is due V. Leipa, who made the measurements. The authors owe thanks also to V. Chang, who prepared the ceramics, and to H. Senecal of the North Campus Instrument Shop, who developed the fabrication technique.

ABSTRACT

A method is developed for measuring the complex dielectric-constant $\epsilon'-j\epsilon''$ of ferroelectric materials in the frequency range 1.8-4.0 kmc. Data are given on the variation of ϵ' and ϵ'' with frequency, temperature, and bias field for a number of ferroelectric ceramics.

FINAL REPORT

CONTRACT NO. DA-36-039 sc-75003

FOREWORD

Since World War II the scope and intensity of research in ferroelectric materials and their applications have steadily increased. Many of these applications have taken advantage of the field-strength dependence of the dielectric constant in ferroelectrics. In the low-frequency range this nonlinear effect has been exploited with varying degrees of success in such applications as dielectric amplifiers, modulators, and memory devices. The ferroelectric capacitor has been quite successfully applied in laboratory work at the Electronic Defense Group in tuning lumped-constant circuits at frequencies as high as 300 mc. In recent years, a microwave interest in ferroelectrics has developed in the wake of intense activity in the field of parametric devices. Ferroelectrics also appear to have likely applications in microwave phase-shifters, and suggestions have been made as to possible microwave applications in power limiters and switches. Their use in delay lines and slow-wave structures may also be anticipated if sufficiently-low-loss materials can be found.

With such a large potential for applications one might naturally ask why the development of these applications has been so slow in

materializing. There are several reasons: the development of ferroelectric materials for microwave applications has yet to be undertaken on a broad front in a systematic way; only a meager amount of information is available on their microwave properties, and the problem of making the necessary dielectric-constant measurements becomes difficult in the microwave range; and, finally, our theoretical understanding of ferroelectricity and the physical mechanism underlying the loss and nonlinear effects is still very limited.

The investigation reported in the following pages has had two principal objectives: the devising of a measurement technique suitable for measuring the complex dielectric-constant of a large number of ferroelectric ceramics over a broad frequency-range; and the investigation of a number of ferroelectric mixtures in the S-band frequency range with regard to variations in frequency, temperature, and bias field. It is not to be inferred that the types of measurements taken are sufficient to characterize the operation of ferroelectrics in any application. Possible parametric applications, for example, would require a knowledge of the mixing properties of ferroelectrics, and any power-limiting application would depend on large-signal effects. The measurements reported here represent only a cursory examination of the small-signal properties of a selected group of ferroelectrics. Nevertheless, it is hoped that this investigation will promote a wider interest in ferroelectrics and their applications in microwave solid-state devices.

1. INTRODUCTION

A knowledge of the relative complex dielectric constant or permittivity, $\epsilon/\epsilon_0 = \epsilon' - j\epsilon''$, of a ferroelectric ceramic under given conditions of frequency, temperature, and bias field is often sufficient to predict its performance in a microwave circuit. However, from the growing list of ferroelectric compounds and mixtures derived from them only a few have been investigated in terms of their dielectric constants in the microwave range. Microwave measurements of the complex dielectric constant of ceramic barium-titanate and some barium-strontium titanate mixtures have been investigated by Powles and Jackson,[1] von Hippel,[2] and Davis and Rubin.[3] Only barium titanate appears to have been investigated in terms of the frequency dependence of the dielectric constant.[2] The frequency spectrum of the ferroelectrics, both single-crystal and polycrystalline forms, is of considerable scientific as well as practical interest. Most of the ferroelectrics measured to date exhibit a relaxation phenomenon at microwave frequencies, broadly occurring in the range of from 1 kmc to 10 kmc. This decrease in the real part of the dielectric constant is still not entirely understood.[4] The physical explanation for this apparently typical phenomenon, when it is found, may represent a major advance in the development of low-loss ferroelectrics for microwave applications.

Of the many ways of measuring dielectric constants in the microwave range only a few are applicable to measuring the very high values typical of ferroelectrics, and these must be modified or used in combination. The fundamental difficulty arises from the fact that the wavelength in the ferroelectric sample is exceptionally small in the microwave range. This not only requires a precise knowledge of the shape

and location of the sample but makes the common assumption of uniform fields in small samples quite inadequate. Reflection methods require the accurate measurement of very high standing-wave ratios and standing-wave phase angles. Transmission methods which require matching the sample with quarter-wavelength sections of known dielectric constant tend to be inaccurate and do not lend themselves readily to spectrum measurements. Cavity resonance and other frequency-determination methods also suffer from one or more of the above disadvantages.

Two methods for making dielectric measurements (denoted A and B in the quarterly progress reports) were studied during the course of this investigation. Since a large number of measurements was anticipated, a special attempt was made to retain those features of previously used methods which would permit the attainment of these objectives with the simplest experimental procedure. Some of the features and underlying philosophy of method A will now be discussed. The method actually employed in making the measurements presented in this report, method B, will be described in detail in the next section.

Method A involves the use of doughnut-shaped samples in a coaxial line configuration such as that shown below. The method of measurement might be termed a network method since the dielectric section of the line is treated as a transmission-line circuit. The parameters of the circuit, which are related to the unknown complex dielectric-constant, are obtained from the characteristics of the image circle for the network. In this case the image circle is the locus of points traced out by the reflection coefficient at the input side of the sample as a sliding short is moved in the line behind the sample.

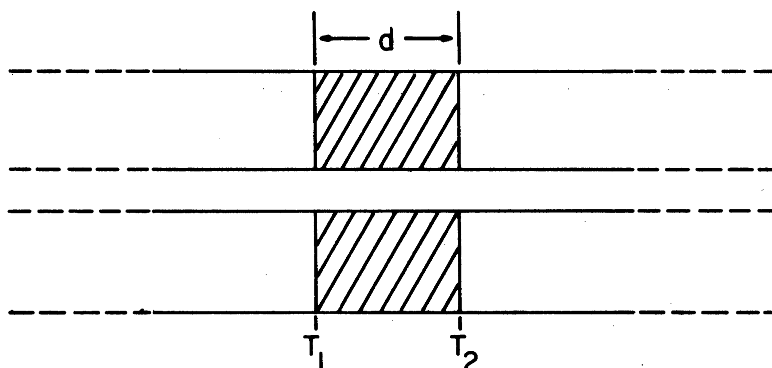

Oliner and Altschuler[5] have proposed such a method in which the image circle is used to obtain the scattering matrix of the network representing the sample. The dielectric constant is then calculated from

$$\epsilon' - j\epsilon'' = \frac{(1-S_{11})^2 - S_{12}^{\;2}}{(1+S_{11})^2 - S_{12}^{\;2}} ,$$

where the scattering coefficients S_{11} and S_{12} are measured relative to the sample faces. This approach to dielectric measurements suffers from the drawback common to most methods when ϵ' is very large; that is, both ϵ' and ϵ'' are very sensitive to phase errors in the measurement of S_{11} and S_{12}. For example, in coaxial systems where relatively large phase errors are often introduced by discontinuities at the connectors, it is possible to obtain meaningless results due to inconsistencies in the measured scattering coefficients even though every possible effort is made to minimize all other sources of error.

With this in mind an approximate procedure was devised which, because of less dependence on phase measurements, might be expected to yield higher precision. The approximation made relates to the location of the center of the image circle when ϵ' is very large. The error due to this approximation is reasonably small for all frequencies if the intrinsic insertion loss through the sample is not allowed to fall below 1 neper. With this assumption, the complex dielectric-constant can be calculated in terms of the location of the center of the image circle in the Γ-plane and the radius of the circle. Both these quantities are relatively independent of standing-wave phase errors since they do not depend on the location of any reference plane or the position of the sample in the line. Another important advantage of this method is the nonexistence of an upper frequency limitation. The derivation of method A and a discussion of the approximation involved appears in Quarterly Progress Report No. 3.

In the last quarter is was found that for some ferroelectrics the error associated with the above-mentioned approximation is not acceptable. This has been remedied by making a higher-order approximation. Preliminary calculations using the revised formulation indicate a very satisfactory convergence. Because of the lack of adequate experimental verification, the method will not be described in this report.

2. METHOD

2.1 General

An impedance or reflection type of measurement was chosen as being the most suitable in view of the objectives outlined above. The

basic procedure for measurements of this type is well known.[6] However, for reasons already discussed, several refinements are required to measure very high dielectric constants.* Included among these refinements is an approximate formula which accounts for the variation of electric field over the face of the sample. As a result of this approximation the impedance method as employed in this investigation and which has been referred to as method B is not exact in the sense that the exact solution for the fields in the sample is known, as in the case of method A. Nevertheless, the error involved in this approximation can be made as small as physical limitations permit and can be readily estimated. The advantages of this method over method A lie in the ease in which temperature and bias variations can be applied to the sample and in the simplicity of fabricating samples. A serious disadvantage arises, however, due to the inherent frequency limitation of the coaxial-type structure and the practical limitation on sample size. For dielectric constants in the order of 4,000 method B probably has a practical upper limit of about 5 kmc.

2.2 Theory

In the impedance method a disk-shaped sample (approximately .020" thick and .030" in diameter) is inserted at the end of a coaxial transmission line as shown in Fig. 1(a). To a first approximation the sample may be represented by a lossy capacitor terminating a uniform transmission line. At frequencies below about 500 mc this approximation works well if the stray capacity at the end of the line is taken into account. One

---

* The impedance method has also been employed successfully by H. Diamond in making microwave dielectric measurements of ferroelectric crystals as well as ceramics. His method is similar in principle to that presented here but differs in detail.

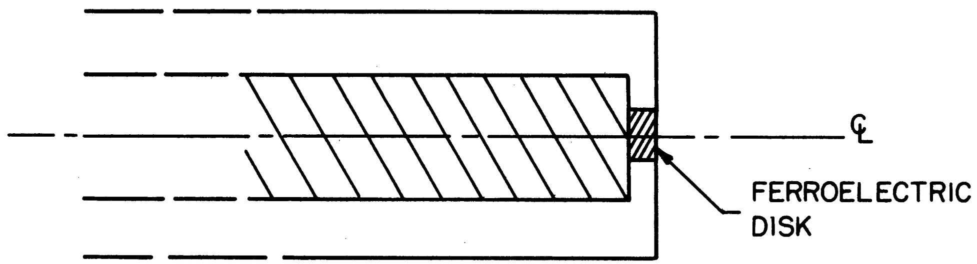

(a) SAMPLE HOLDER GEOMETRY

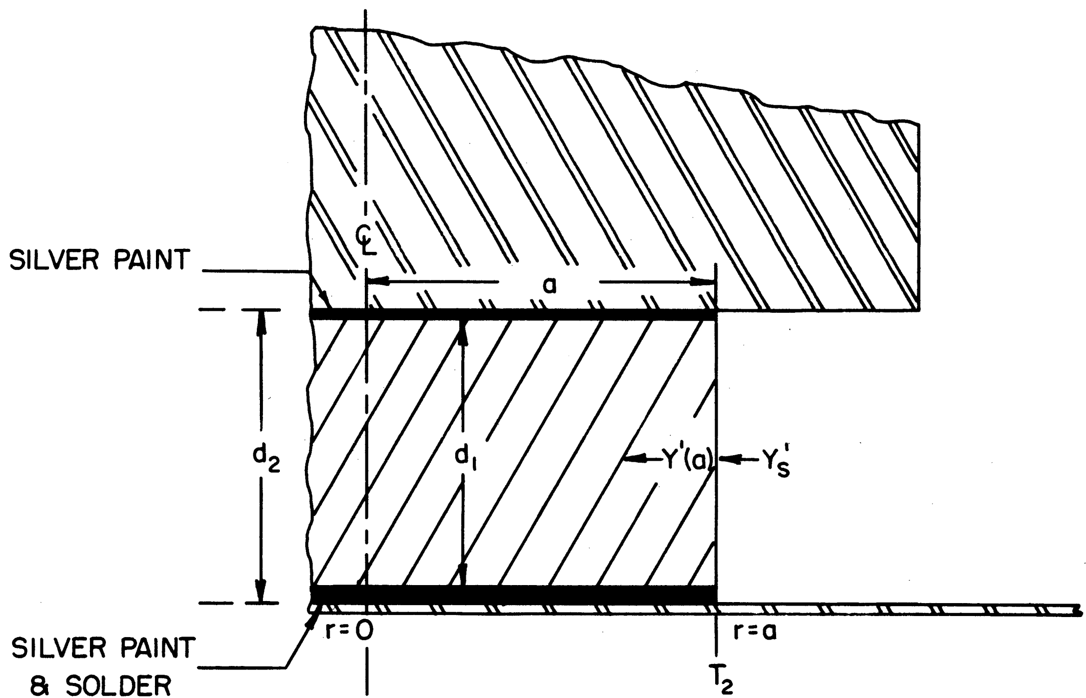

(b) DETAIL OF FERROELECTRIC SAMPLE

FIG. 1 SAMPLE AND SAMPLE HOLDER

can then determine ϵ' and ϵ'', knowing the impedance at the capacitor terminals. At higher frequencies this procedure breaks down in several respects. It becomes no longer possible to identify the terminals of the effective capacitance since the fringing fields are no longer negligible. Also, the apparent capacity of the sample cannot be simply related to the complex dielectric-constant because of the nonuniform variation of the electric field throughout the sample.

These difficulties were overcome by considering the sample disk as a section of radial line. The radial line mode will be the only mode excited in the sample if the thickness of the sample is small compared to the wavelength in air. The thick center conductor permits the higher-order modes generated in the vicinity of the corner to attenuate before reaching the sample. This allows one to establish a reference plane T_2 for the equivalent circuit at the sample-air interface as shown in the expanded view of the sample in Fig. 1(b). The normalized admittance Y'_s looking into the sample at T_2 can be calculated in terms of the complex dielectric-constant of the sample by radial-line theory. The remaining problem is to relate Y'_s to the measured admittance Y'_m at some chosen reference plane T_1 in the slotted line preceeding the sample holder. This is done by noting that, at any two reference planes where only the dominant mode propagates, any two-port lossless network can be represented by the equivalent circuit shown in Fig. 2, where Y'_1 and Y' are normalized susceptances and n is real.[7] If T_1 is located at a null when the sample is replaced by a metal disk of the same size, then $Y'_1 = \infty$. The remaining elements of the equivalent circuit must be determined at each frequency. This is most easily done by replacing the sample with two known dielectrics. Rutile (TiO_3) and

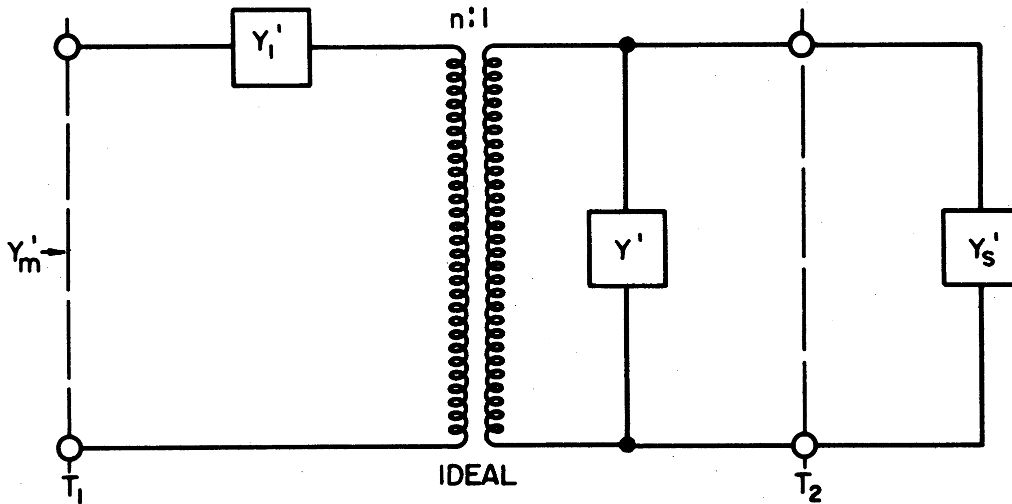

FIG. 2 EQUIVALENT CIRCUIT FOR SAMPLE HOLDER

air have proved satisfactory for this purpose. In the case of rutile it is assumed that there is negligible dispersion in the dielectric constant from 250 mc, where the measurement is made, to 4 kmc. Then

$$Y'_s = n^2 Y'_m - Y' \tag{1}$$

where

$$Y'_m = \frac{\rho(1 + \tan^2 \frac{2\pi\Delta}{\lambda}) - j(\rho^2 - 1) \tan \frac{2\pi\Delta}{\lambda}}{1 + \rho^2 \tan^2 \frac{2\pi\Delta}{\lambda}}, \tag{2}$$

and ρ is the measured voltage standing-wave-ratio when the line is terminated in the sample. The distance Δ measures the shift in the standing-wave minimum toward the generator when the sample is replaced by a metal short.

It should be noted that the equivalent circuit accounts for not only the fringing fields in the sample holder but also for all other discontinuities in the line between the reference planes, including the connectors and the tapered section.

It remains to relate Y'_s to the complex dielectric-constant of the sample. Considering the sample as a section of radial line in which a voltage maximum occurs at the load ($r_o = 0$), one may calculate the normalized input admittance $Y'(r)$ at a radius r, <u>looking in the direction of decreasing radius</u>, from the following equation:[8]

$$Y'(r) = \frac{-j}{Ct(x,y)} , \qquad (3)$$

where the load admittance $Y'(r_o)$ has been taken to be zero and $Ct(x,y)$ is defined by

$$Ct(x,y) = \frac{J_1(y)N_0(x) - N_1(y)J_o(x)}{J_1(x)N_1(y) - N_1(x)J_1(y)} , \qquad (4)$$

and

$$x = k'r, \quad y = k'r_o .$$

The constant k' is the wave number in the sample and can be written,

$$k' = (2\pi/\lambda)\sqrt{\epsilon' - j\epsilon''} . \qquad (5)$$

Since, as $r_o \rightarrow 0$,

$$\lim_{y \rightarrow 0} Ct(x,y) = -\frac{J_o(x)}{J_1(x)} , \qquad (6)$$

it follows that at $r = a$,

$$Y'(a) = j\frac{J_1(k'a)}{J_o(k'a)} . \qquad (7)$$

At any radius the actual admittance $Y(r)$ is related to the normalized admittance $Y'(r)$ by

$$Y(r) = Y_o(r)Y'(r) , \qquad (8)$$

where the characteristic admittance of the radial line at the radius r, $Y_o(r)$, is given by

$$Y_o(r) = \frac{2\pi r}{d}\sqrt{\frac{\epsilon}{\mu_o}} , \qquad (9)$$

and d is the height of the line. Referring to Fig. 1(b), the height of the line within the sample, d_1, is different from that outside the sample, d_2 owing to the thickness of silver plating and solder which is applied in mounting the sample. In the sample holder to be described, $d_1 = .019''$ and $d_2 = .0205''$. The boundary condition to be satisfied at the air-dielectric interface is $Y(a) = Y_s$, where Y(a) is the admittance in the sample at r = a and Y_s is the admittance in air at r = a. It follows from (8) and (9) that

$$Y'(a) = \frac{d_1}{d_2} \frac{1}{\sqrt{\epsilon' - j\epsilon''}} Y_s' . \qquad (10)$$

Using (5) and (7) this may be written at x = k'a as

$$w = x\frac{J_1(x)}{J_o(x)} = -j\frac{d_1}{d_2}\left(\frac{2\pi a}{\lambda}\right)Y_s' , \qquad (11)$$

where w is known and x is to be determined.

w can be represented by a continued fraction:[9]

$$w = \cfrac{2(x/2)^2}{1 - \cfrac{(x/2)^2}{2 - \cfrac{(x/2)^2}{3 - \cfrac{(x/2)^2}{4 - \ddots}}}} \qquad (12)$$

Terminating (12) with the terms shown leads to a quadratic in x^2,

$$x^2 = \frac{72w + 192 - \sqrt{(72w + 192)^2 - (w + 12)1536w}}{2(w + 12)} . \tag{13}$$

Since

$$\epsilon' - j\epsilon'' = x^2\left(\frac{\lambda}{2\pi a}\right)^2 , \tag{14}$$

Equation (13) yields the desired expression for the complex dielectric-constant:

$$\epsilon' - j\epsilon'' = 12 \left(\frac{\lambda}{2\pi a}\right)^2 \left[\frac{b'-jb''-\sqrt{(b')^2-(b'')^2-c'-j(2b'b''-c'')}}{u + 12 - jv}\right] . \tag{15}$$

$$w = u - jv$$

$$b' = 3u + 8 \;\; ; \;\; b'' = 3v$$

$$c' = \frac{8}{3}(u^2 + 12u - v^2); \;\; c'' = \frac{16}{3}v(u+6) .$$

This approximation is good to within 1% for real x less than 2.2, which is considerably less than the error obtained with a Taylor series approximation. It is primarily this limit on $x = k'a$ which places an upper frequency-limit of about 5 kmc on this method for dielectric constants in the order of 4,000. In this connection, a great deal depends on the precision with which the samples can be fabricated, since the sample radius is directly involved along with the frequency in determining the maximum acceptable value of x.

2.3 Experimental Equipment and Procedure

Figure 3 is an assembly drawing of the sample holder. The purpose of the tapered section is to minimize the effect of position errors in the standing-wave measurement of Y_m'. It can be shown that for a given deviation in the measurement of the standing-wave minimum, the least error in the measured susceptance occurs when that susceptance

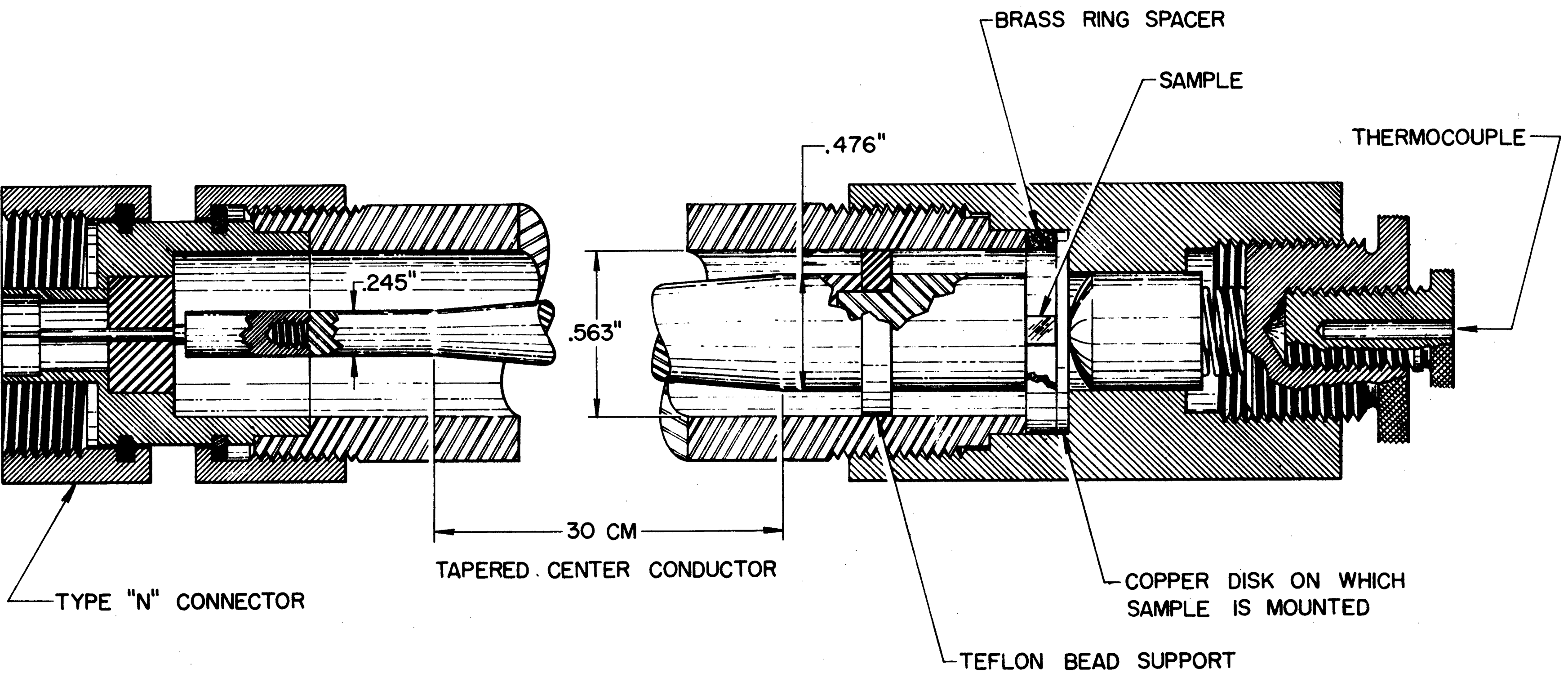

FIG.3 SAMPLE HOLDER ASSEMBLY

is equal to the characteristic admittance of the slotted line. The taper shown provides a five-to-one admittance transformation, which represents a reasonable compromise for many ferroelectrics in the S-band range. The taper itself was designed using the method of Willis and Sinha.[10]

Heat for the temperature measurements is applied to the sample by means of a chromel-wire coil wound on a ceramic tube which encloses the entire sample holder. Temperatures below room temperature are obtained by enclosing the sample holder in dry ice. The temperature of the sample is measured under essentially equilibrium conditions by means of a thermocouple attached to the interior plug behind the sample.

The disk-shaped samples are fabricated in the following manner. Using a diamond wheel, a ceramic sheet is first cut from the rough sample stock to the approximate thickness. After surface grinding to the d_1 (0.019") dimension, this sheet is painted on both sides with Dupont No. 4731 silver paint, baked at $600^{\circ}C$ for 22 minutes, and furnace cooled. The painted sheet is then resurfaced to a combined electrode thickness of 0.001". The individual samples are cut from this sheet with an ultrasonic cutter and then carefully centered and soldered on a thin (0.005") flexible copper disk. This disk supports the sample in the holder, and the spring-loaded plug pressing against its back in the assembled sample holder assures contact between the sample and the center conductor.

Figure 4 is a schematic diagram of the experimental setup. Two slotted lines (Hewlett-Packard 805A) were employed, one for making the admittance measurements of Y'_m and the other for resetting the frequency of the signal generator. The latter was required because the

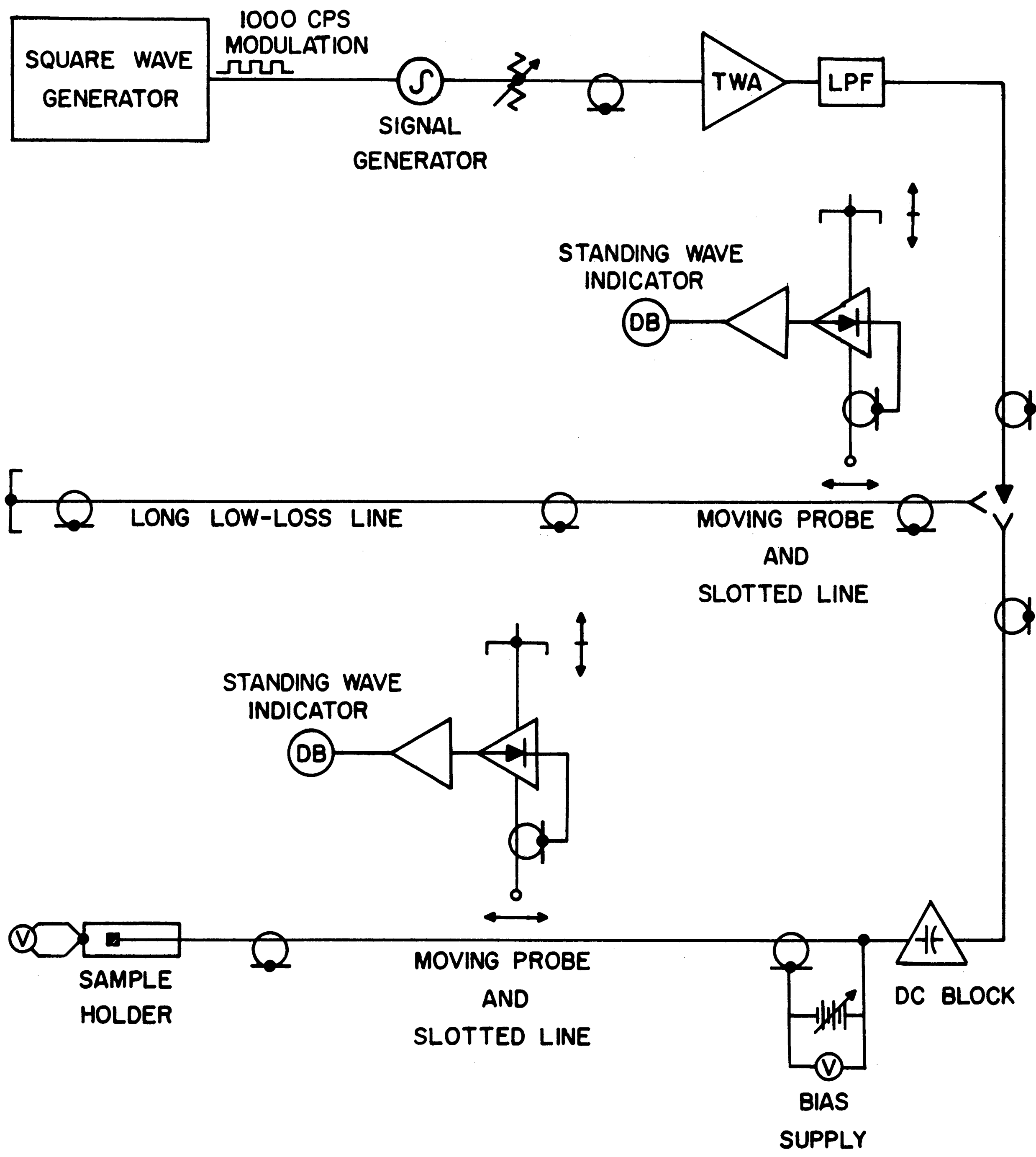

FIG.4 EXPERIMENTAL ARRANGEMENT FOR THE MEASUREMENT OF THE COMPLEX DIELECTRIC-CONSTANT OF FERROELECTRICS.

parameters of the equivalent circuit are quite sensitive to frequency changes. The wavelength λ used in the calculations was measured in the first slotted line. Both lines were modified with a 40-1 lead-screw drive on the carriage. Dial gauges, specially ordered from the Ames Company, were used on both lines. These gauges have a 15 cm range with graduations of 0.01 mm.

Two methods were successfully employed in making the vswr measurements. The first is basically an RF substitution technique which was generalized to permit the use of arbitrary amounts of attenuation.[11] Since vswr's in the range of 50-100 were commonly encountered, a 10 db calibrated attenuator was usually employed in this method. The second method, which gave results in very close agreement with the first, is due to Winzemer.[12] Both techniques give the vswr independently of the detector characteristics. In addition, Winzemer's method does not require a calibrated attenuator. The traveling-wave-tube amplifier shown in the diagram was needed to obtain a sufficient signal level at the standing-wave minimum.

3. DISCUSSION OF RESULTS

The temperature variation of the complex dielectric-constant of several selected ferroelectrics is plotted in Figs. 5-11 for the zero-bias condition. In Figs. 12-41, ϵ' and ϵ'' for a larger variety of materials are plotted versus frequency and bias field at room temperature (26°C). Mixtures are referred to in mole percent. All the ferroelectrics investigated, with the exception of the following, were prepared and

fired in the University of Michigan Solid State Devices Laboratory. The Hi-Q-91 mixture is a commercial ceramic, kindly provided by the Aerovox Corporation. The $BaTiO_3$-$PbTiO_3$ and $SrTiO_3$-$PbTiO_3$ mixtures were purchased from the Centralab Division of the Globe Union Corporation. The hot-pressed $BaTiO_3$ and $Cd_2Nb_2O_7$ materials were generously supplied by Dr. A. deBrettville of the U. S. Army Signal Research and Development Laboratories. As the word implies, these ceramics were fired under high pressure (5000 psi) and for this reason are more dense than ceramics fired at atmospheric pressure.

Referring to Fig. 5, the dielectric constant of pure $BaTiO_3$ exhibits the characteristic behavior versus temperature at 3 kmc which has been reported by Powles and Jackson at 9.45 kmc.[13] However, the dispersion characteristic shown in Fig. 12 shows a leveling-off at 4 kmc which suggests that a somewhat higher value would be obtained at 9.45 kmc than that reported by Powles and Jackson. This leveling-off of the relaxation at or before 4 kmc is typical of almost all the materials measured. The hot-pressed $BaTiO_3$ reported in Figs. 6, 14, and 15 differs from the common material in several respects. The Curie peak in ϵ' and ϵ'' is lowered, but the values off the Curie peak are raised. The loss tangent is essentially the same for the two cases. However, the variation of ϵ' with bias field (hereafter referred to as the tunability) for the hot-pressed sample is considerably less than that for ordinary $BaTiO_3$. It should be mentioned that the hot-pressing process establishes a plane of polarization in the sample at right angles to the applied electric field. Thus, if the samples were cut from the raw material so as to place the spontaneous moment parallel to the applied field, different results might be expected.

The addition of only a small percentage (0.05%) of Fe_2O_3 to $BaTiO_3$ results in two interesting effects. Referring to Fig. 7, a subsidiary peak in the temperature curve is introduced at 25°C, while the principal Curie peak at 120°C is suppressed. In Fig. 16 the imaginary part of the dielectric constant ϵ'' is seen to decrease with frequency in contrast to a rising characteristic for all other materials investigated.

It is well known that the addition of Sr to $BaTiO_3$ lowers the Curie point. This behavior is apparent in Figs. 9-11. The corresponding bias characteristics reflect this shift. In general all ferroelectrics will exhibit their strongest tunability at or near the Curie temperature. The Mn and Ni mixtures and the 1% Fe_2O_3 mixtures in Figs. 22-29 have been proportioned to have Curie points at or near room temperature. The addition of these materials to $BaTiO_3$ modifies the tunability characteristic somewhat but primarily seems to influence the frequency behavior of ϵ' and ϵ''. The addition of either Mn or Fe_2O_3 to the Ba-Sr base can result in almost a total lack of dispersion in the frequency range of 1.8-4.0 kmc. It is probable that the relaxation frequency is lowered by this addition. One of the advantages gained by the use of metal additives is a sharper tunability characteristic. For example, compare Fig. 25 with Fig. 31. Both mixtures have a Curie peak at 26°C.

$PbTiO_3$ (see Figs. 34 and 35) exhibits no tunability at all at room temperature. This is not unexpected since its Curie point is quite high (490°C). When 4% $PbTiO_3$ is added to $BaTiO_3$ the tunability of the resulting mixture is substantially less than that obtained from the pure $BaTiO_3$ as shown in Fig. 33. This material is widely used in

piezo-electric transducers but appears not to have particularly useful properties in the microwave range. On the other hand, when 35% $PbTiO_3$ is mixed with 65% $SrTiO_3$ to obtain a Curie point at 28°C, an excellent tunability characteristic is obtained (Fig. 37). This would be expected from the sharp Curie peak in the temperature characteristic shown in Fig. 8. $Cd_2Nb_2O_7$ does not exhibit any tunability at room temperature (Fig. 39), having a Curie point at -113°C. However, it may be useful as a constituent in a ferroelectric mixture owing to its exceptionally low-loss characteristic. Figure 38 shows a loss tangent of less than $\tan \delta = 0.05$ at 3 kmc. The commercial Hi-Q-91 material has a good tuning characteristic but a relatively high loss-tangent in the S-band range.

4. CONCLUSIONS

Ferroelectrics appear to retain all their small-signal properties up to at least 4 kmc. A relaxation in the real part of the dielectric constant occurs usually at 4 kmc or lower. This relaxation is accompanied by an increase in the loss tangent. None of the materials investigated, with the exception of $Cd_2Nb_2O_7$, exhibited a $Q = (\tan \delta)^{-1}$ of more than 10 throughout the range of temperature, frequency,and bias variations.

Measurements are very much needed up through the X-band range before any general statements regarding the relaxation phenomenon can be made. From the cursory study reported here it seems conceivable that ferroelectrics might be found for which the loss at X-band and perhaps higher frequencies is not particularly greater than that in the S-band range. Although the loss figures reported in this frequency range are

not especially encouraging from an applications point of view, there does seem to be some hope of obtaining improved performance with more optimum mixtures. A more thorough study of $Cd_2Nb_2O_7$ and mixtures derived from it would seem to be justified in this regard. Finally, tri-ponent mixtures involving small percentages of the heavy metals and their oxides seem to offer interesting possibilities for some applications.

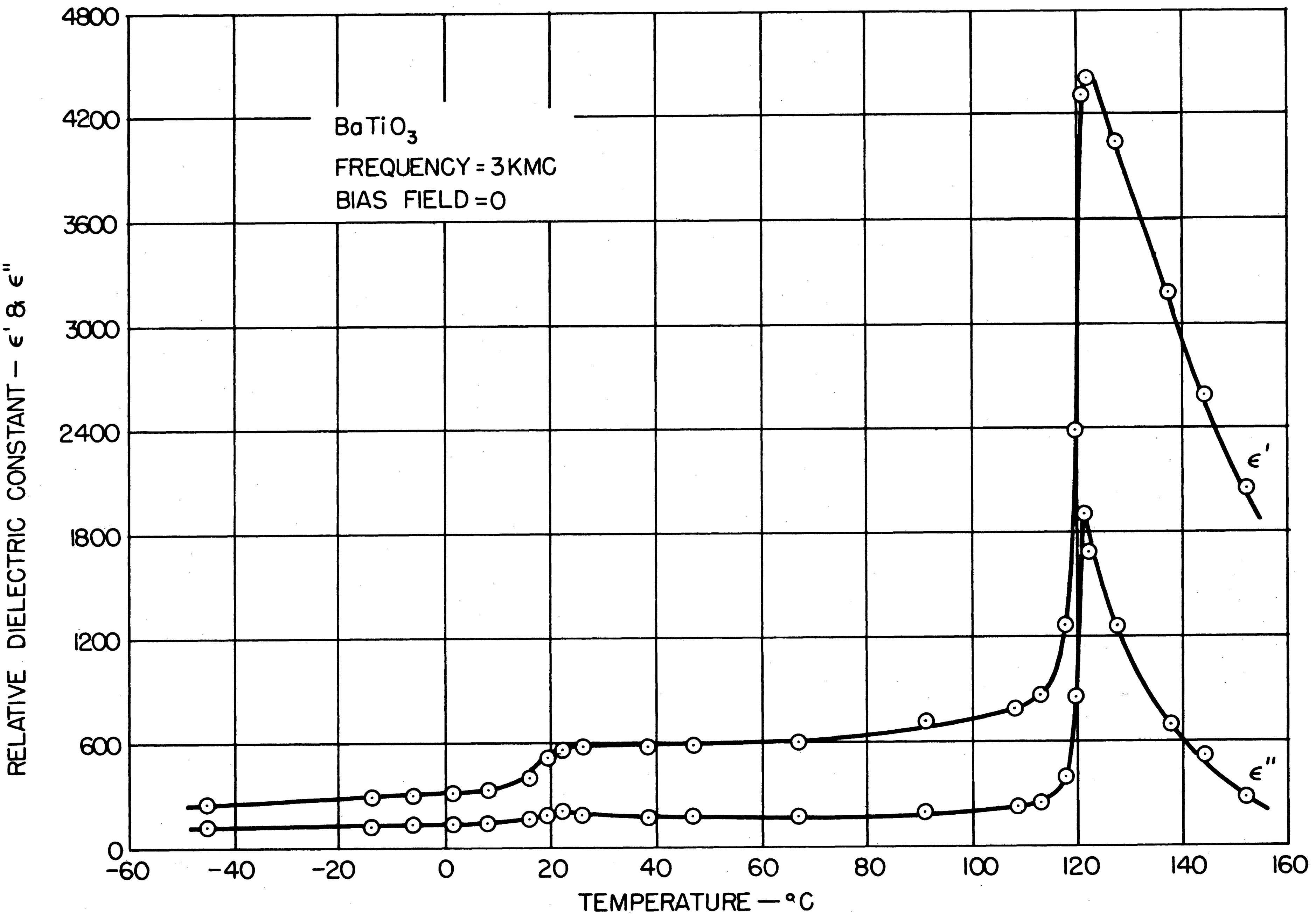

FIG. 5 RELATIVE DIELECTRIC CONSTANT VS TEMPERATURE

EA 33

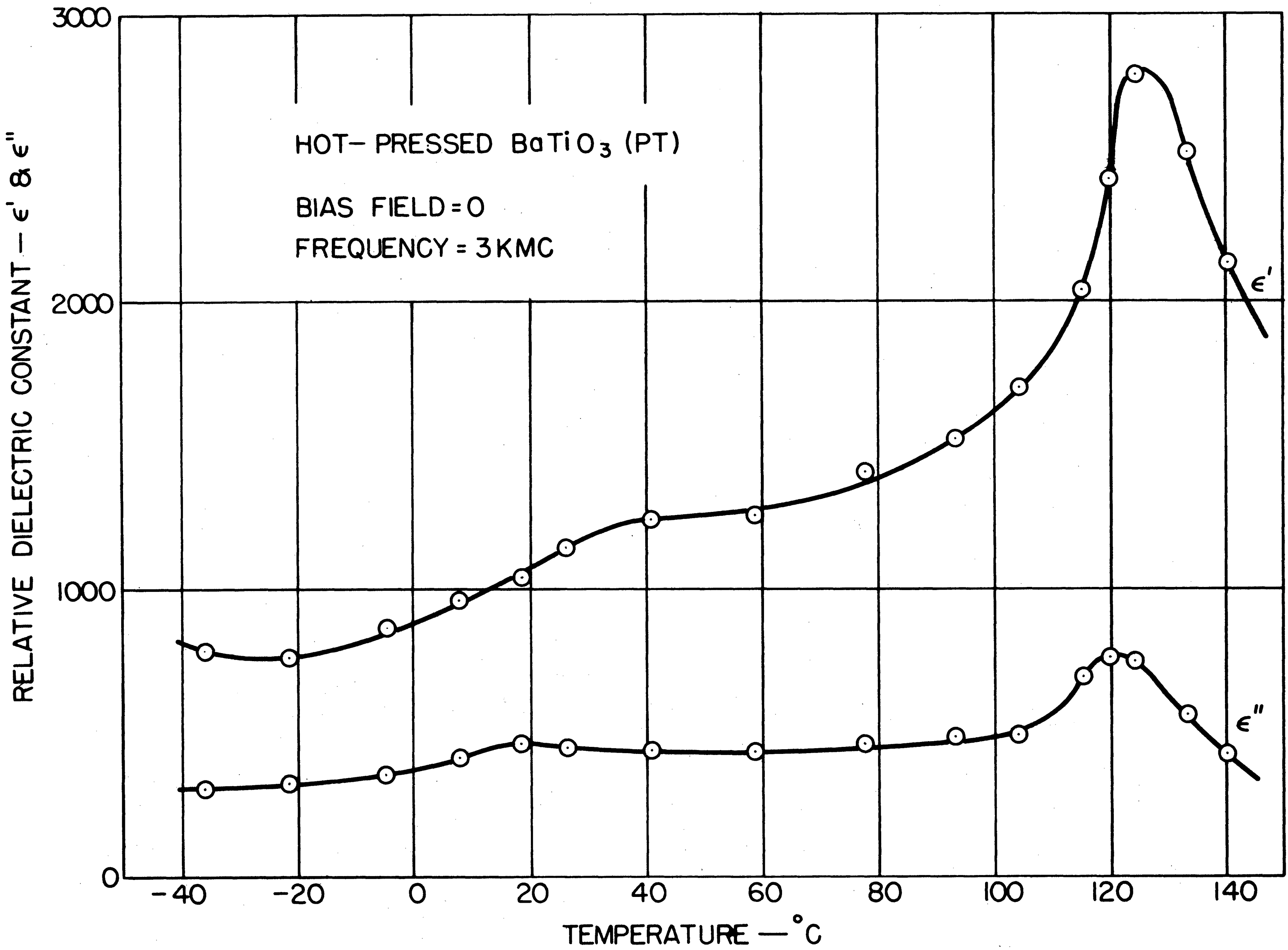

FIG. 6 RELATIVE DIELECTRIC CONSTANT VS TEMPERATURE

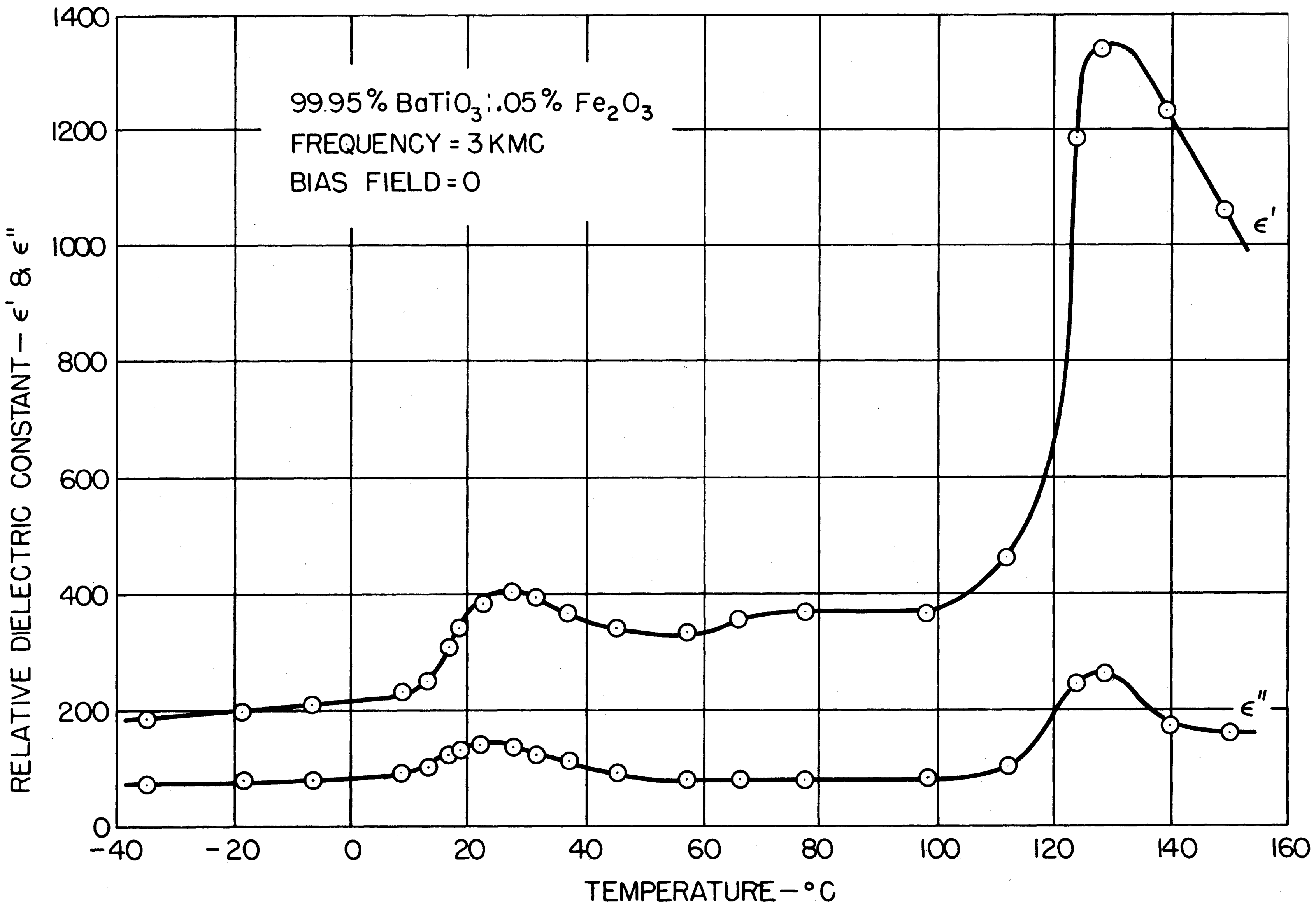

FIG. 7 RELATIVE DIELECTRIC CONSTANT VS TEMPERATURE

FA32

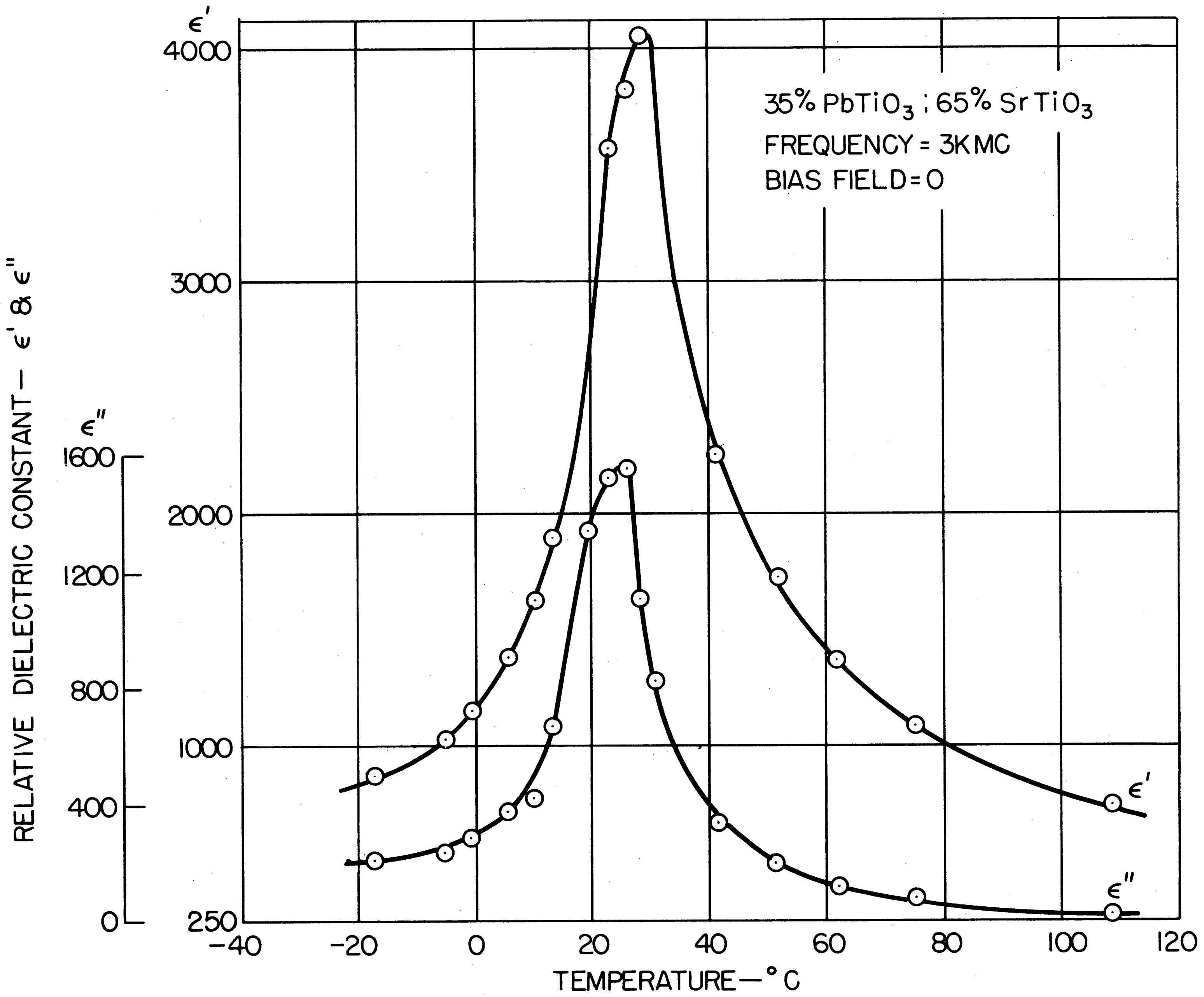

FIG.8 RELATIVE DIELECTRIC CONSTANT VS TEMPERATURE

EA 37

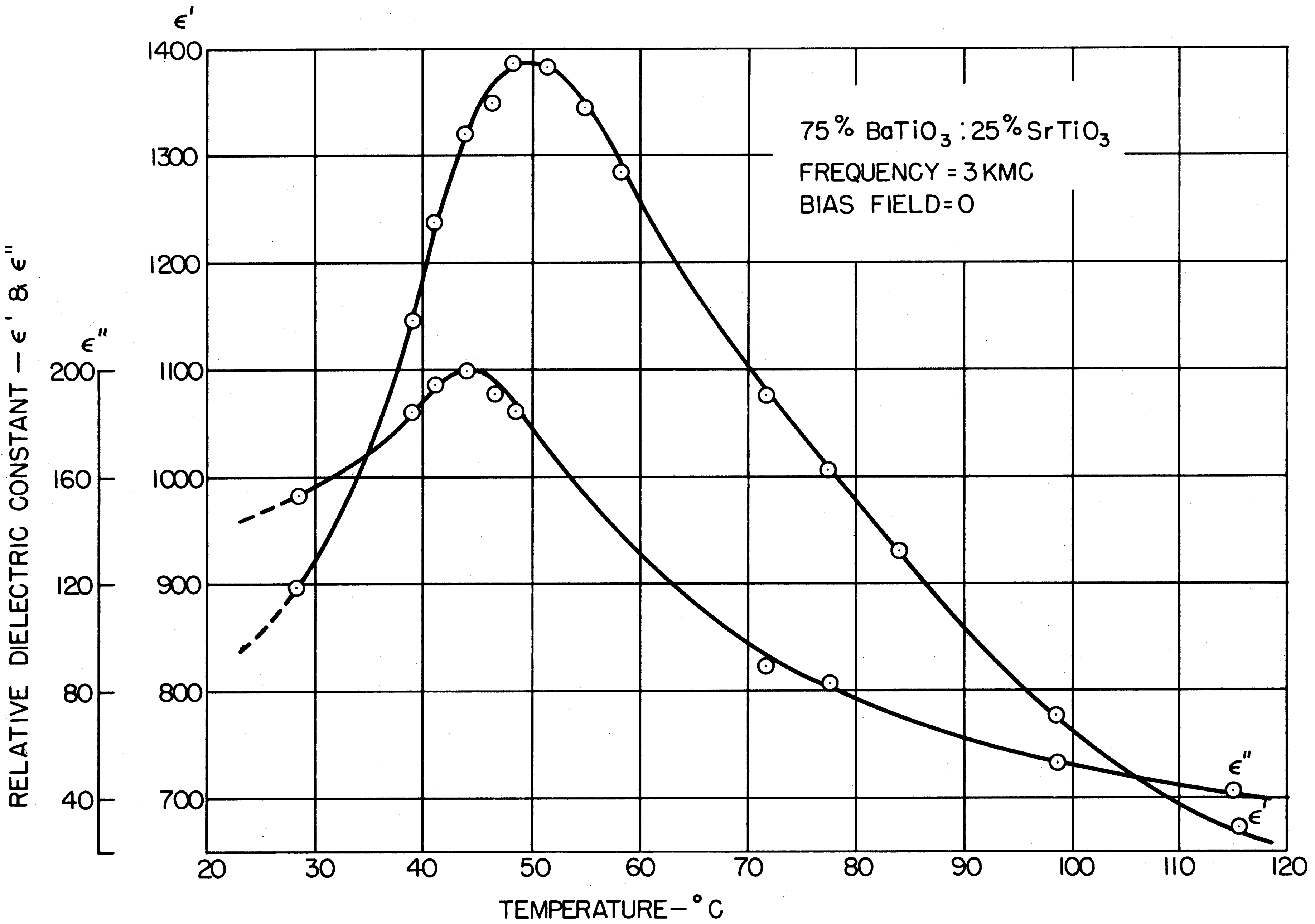

FIG. 9 RELATIVE DIELECTRIC CONSTANT VS TEMPERATURE

FA34

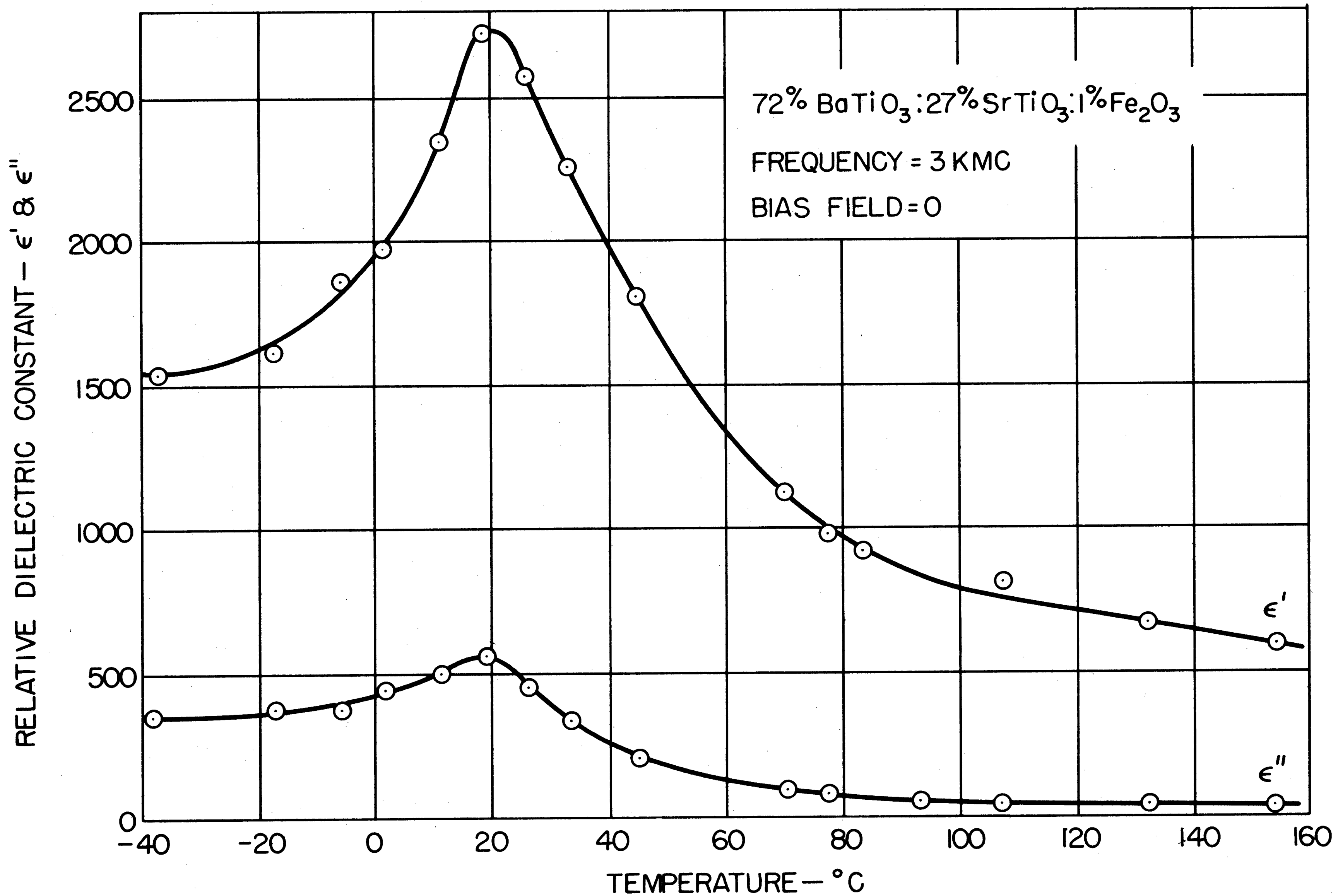

FIG. 10 RELATIVE DIELECTRIC CONSTANT VS TEMPERATURE

EA 39

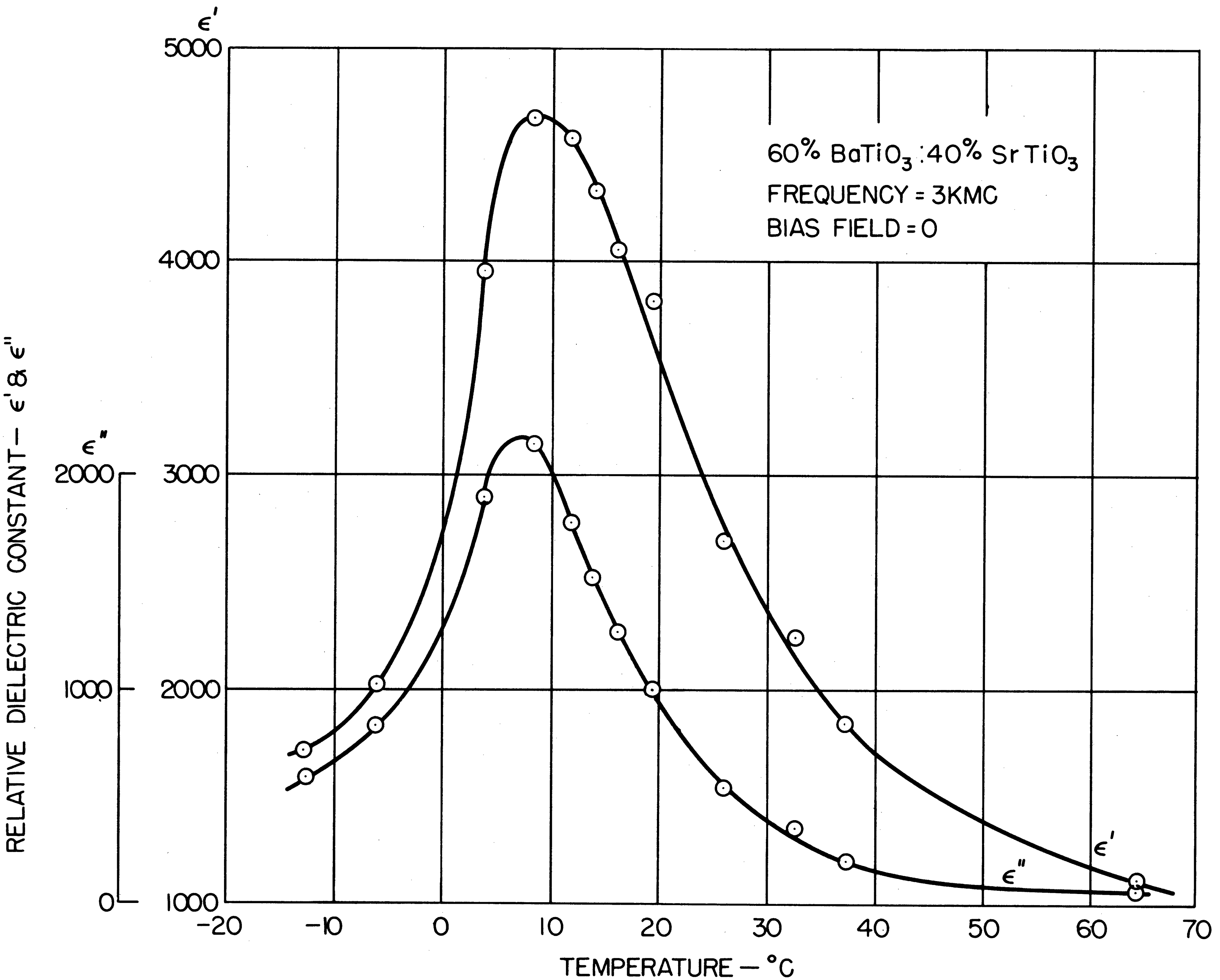

FIG.11 RELATIVE DIELECTRIC CONSTANT VS TEMPERATURE

EA35

This page has been left blank in order that the following figures may be shown in logical pairs.

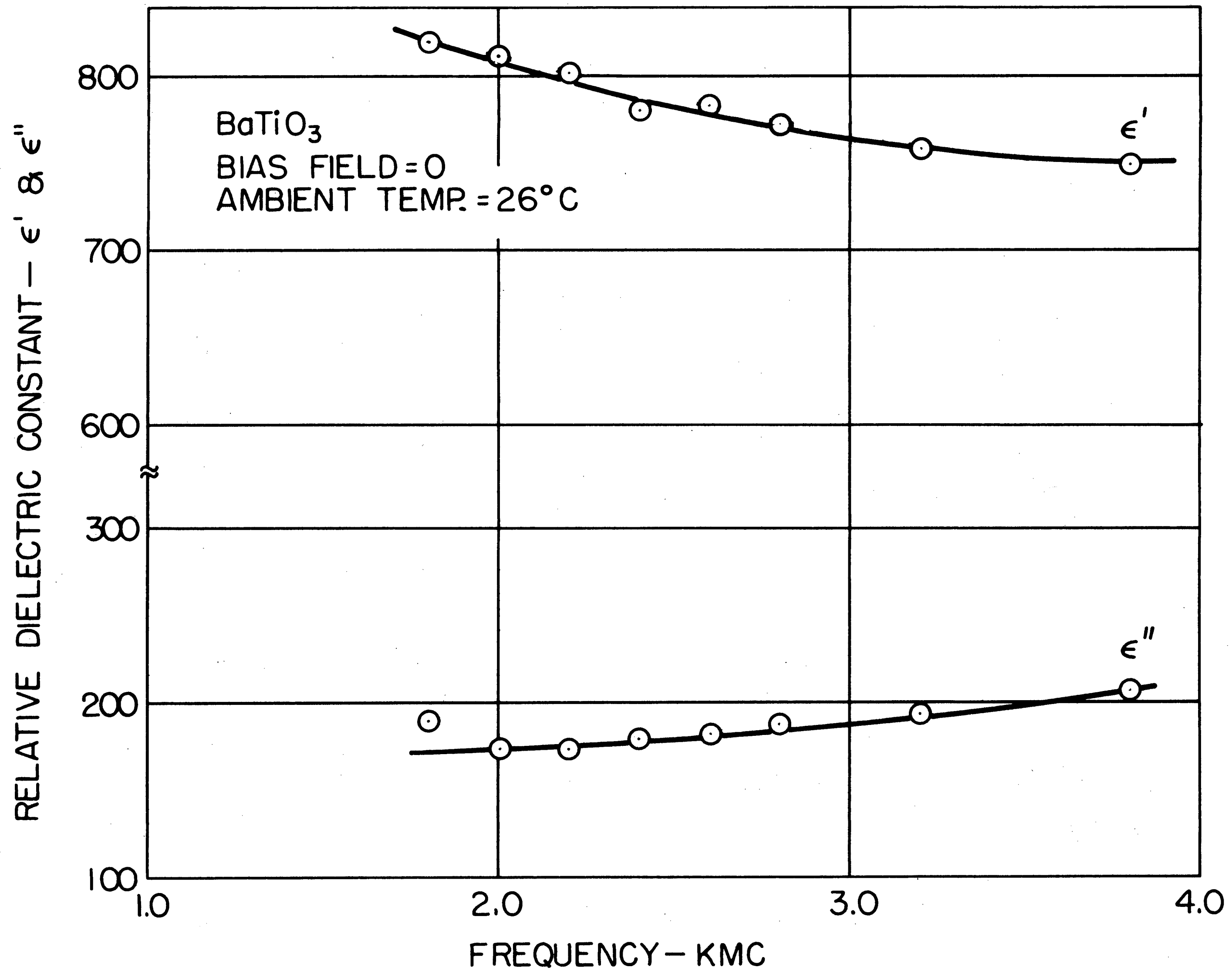

FIG. 12 RELATIVE DIELECTRIC CONSTANT VS FREQUENCY

EA 13

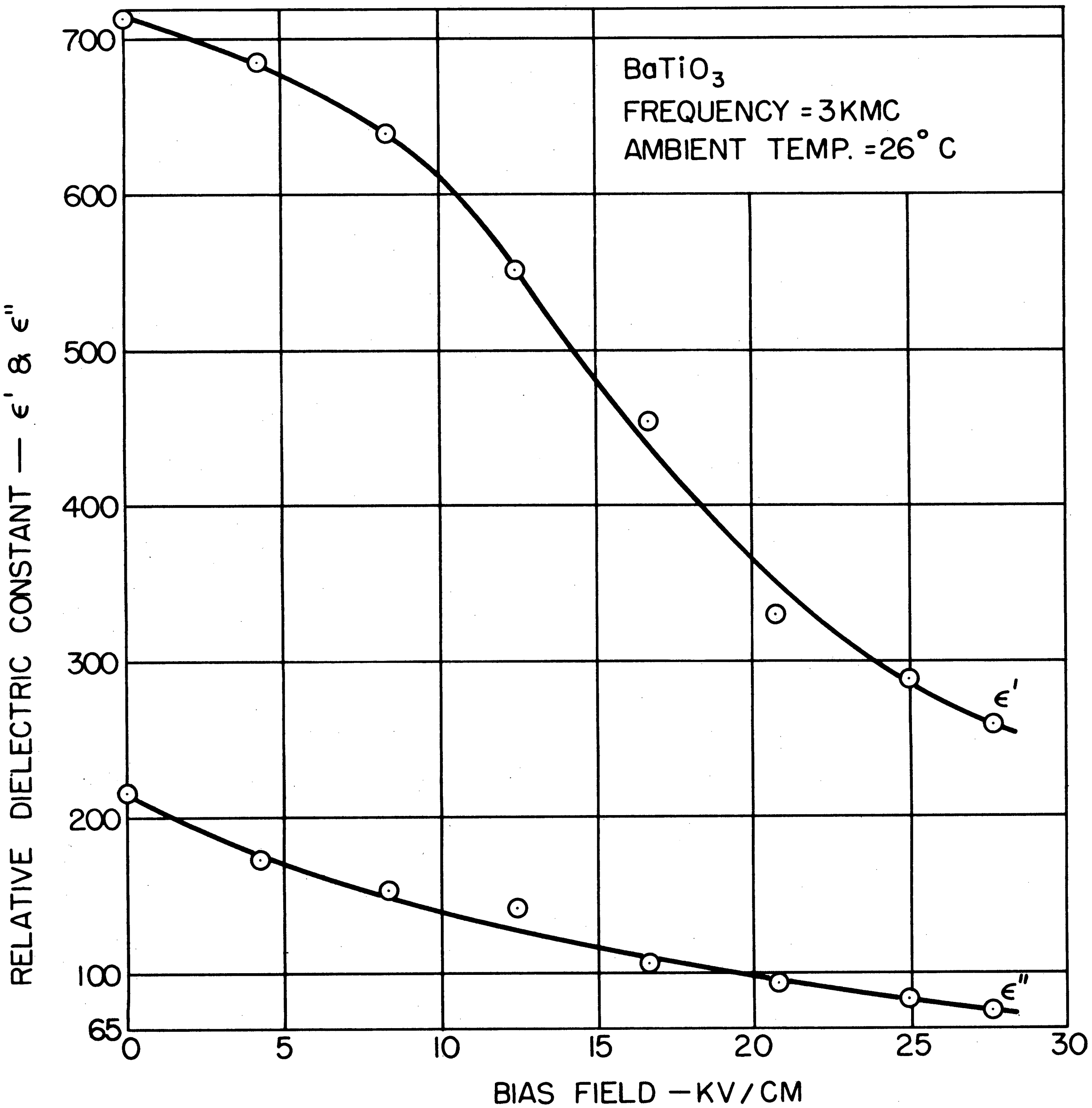

FIG. 13 RELATIVE DIELECTRIC CONSTANT VS BIAS FIELD

AD47

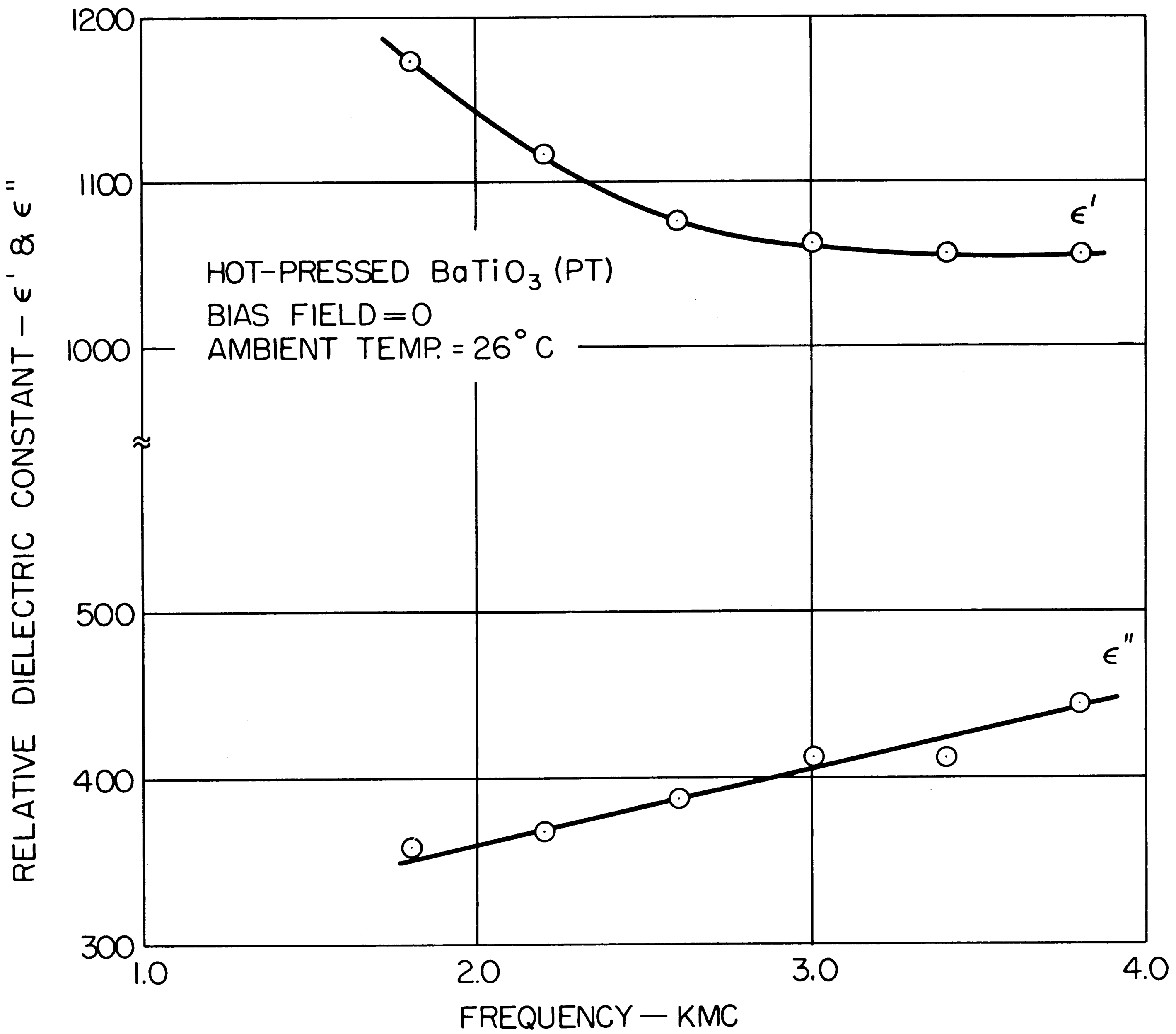

FIG. 14 RELATIVE DIELECTRIC CONSTANT VS FREQUENCY

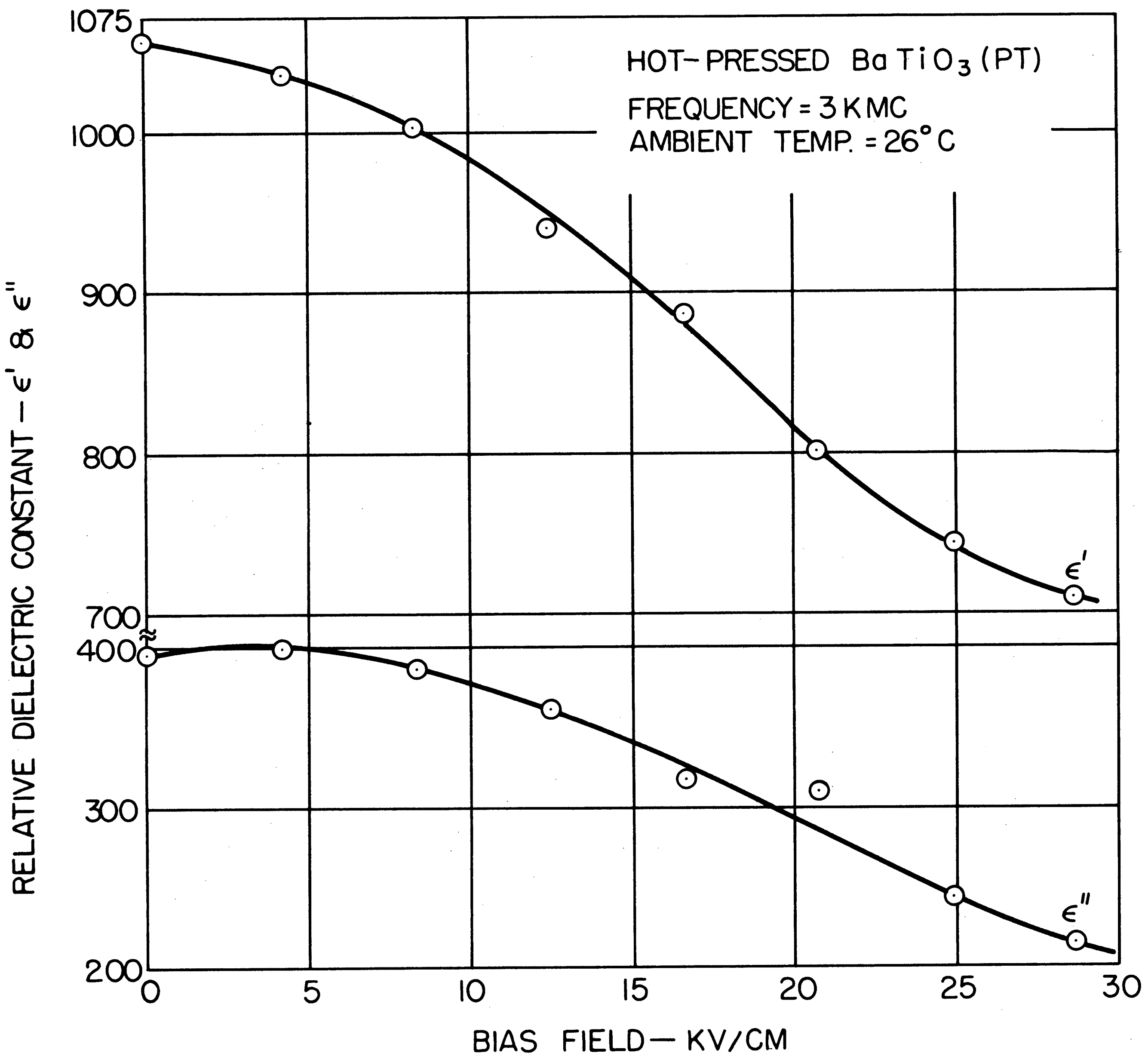

FIG. 15 RELATIVE DIELECTRIC CONSTANT VS BIAS FIELD

EA7

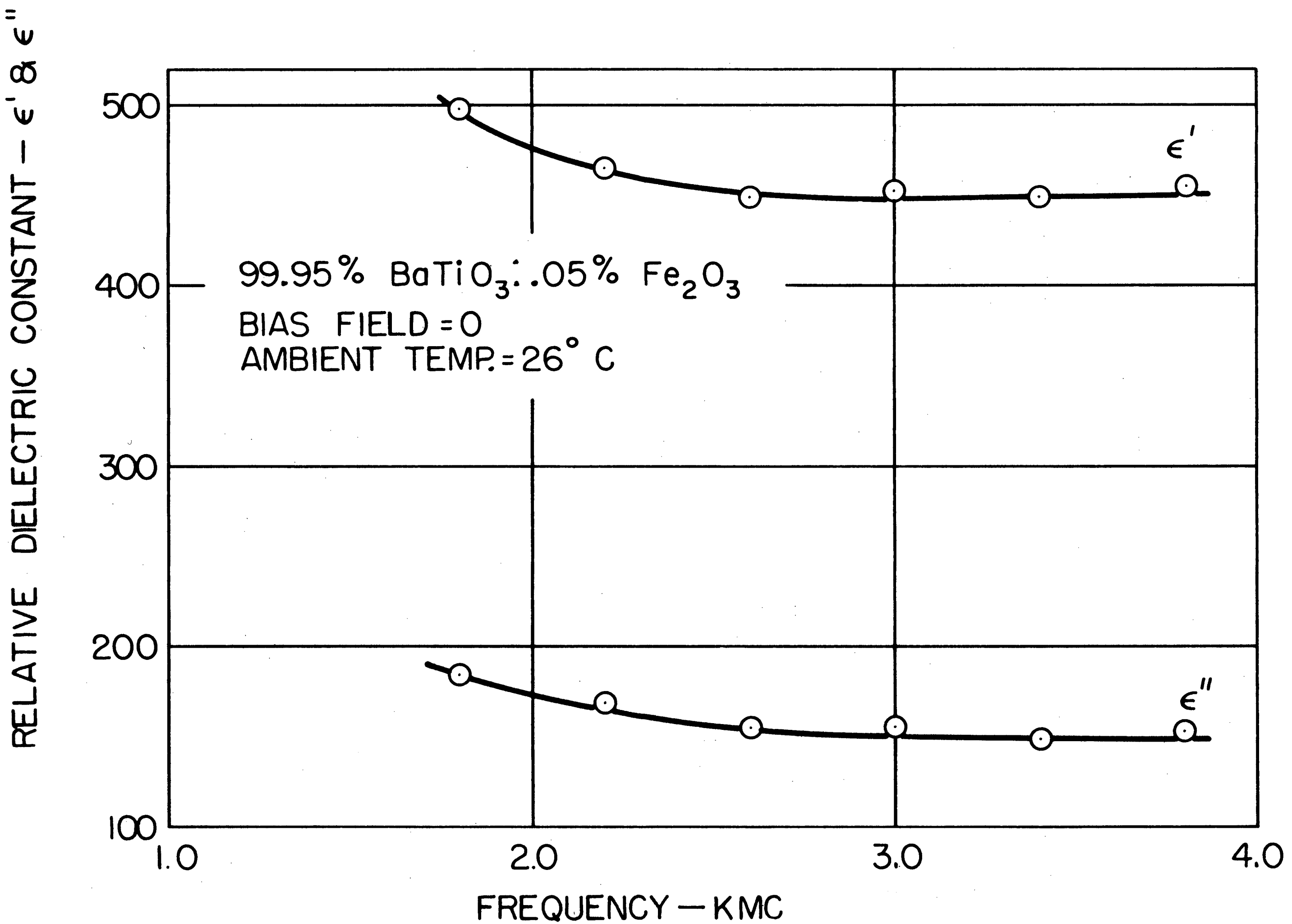

FIG.16 RELATIVE DIELECTRIC CONSTANT VS FREQUENCY

EA16

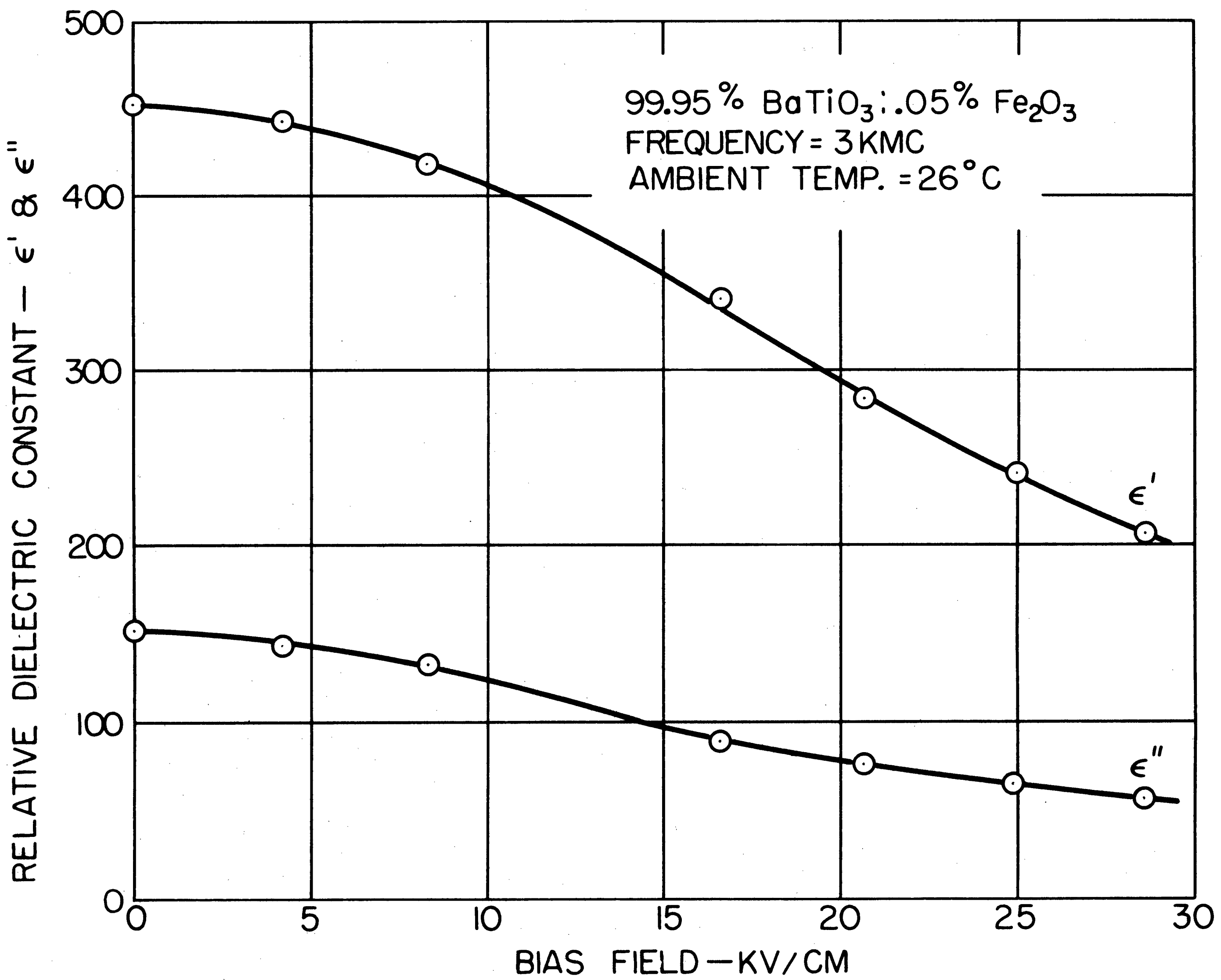

FIG. 17 RELATIVE DIELECTRIC CONSTANT VS BIAS FIELD

EA18

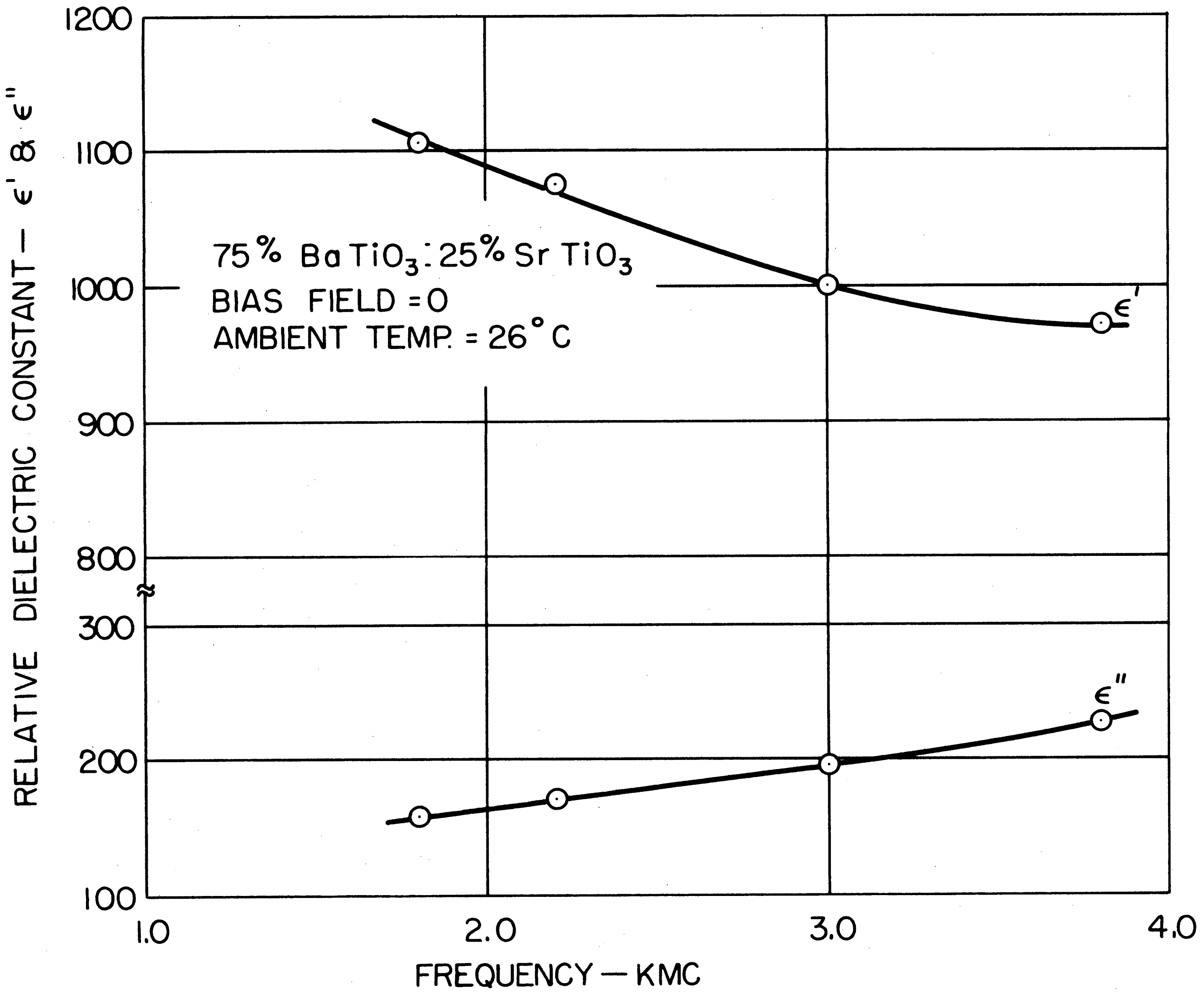

FIG. 18 RELATIVE DIELECTRIC CONSTANT VS FREQUENCY

EA15

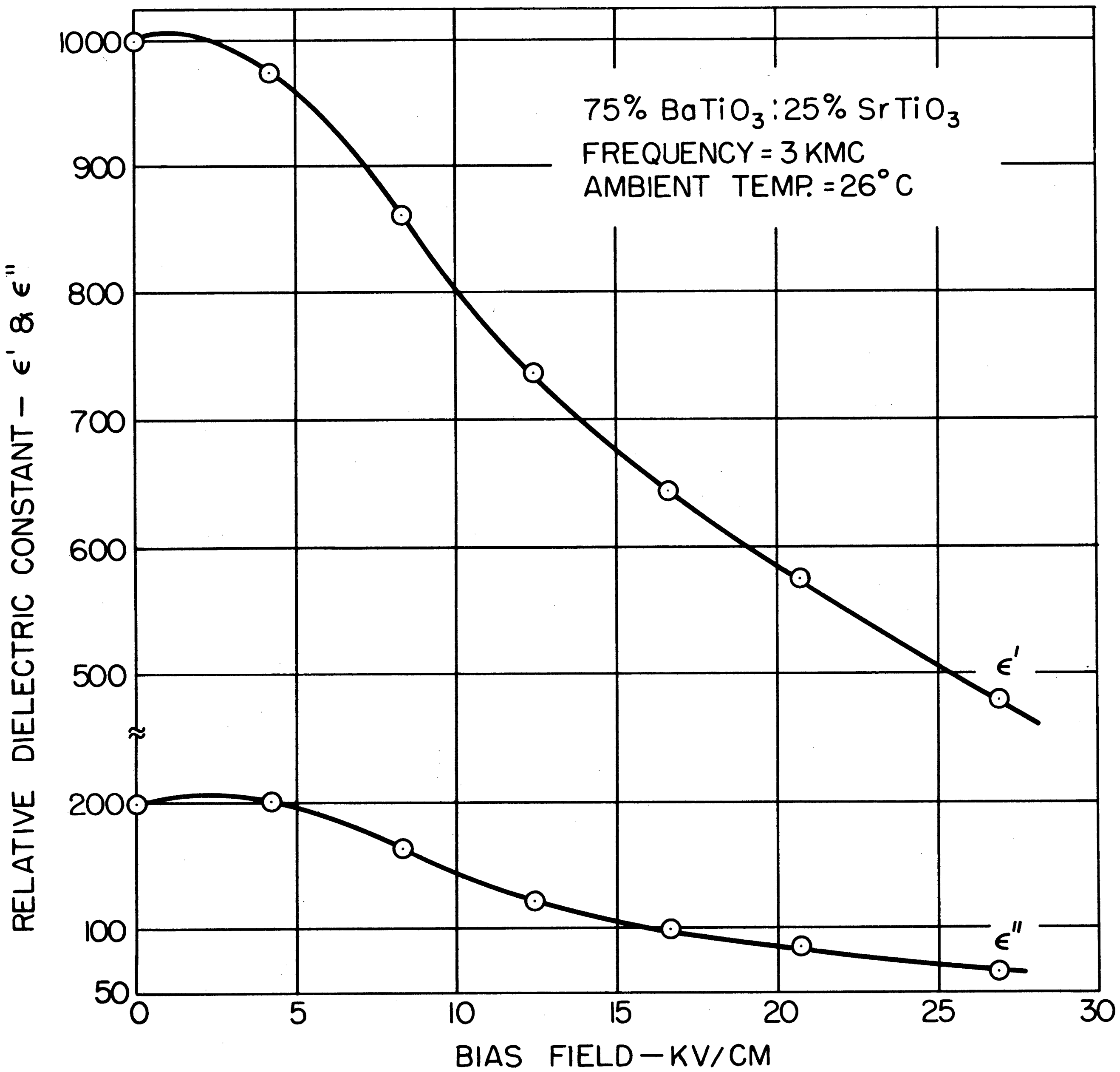

FIG. 19 RELATIVE DIELECTRIC CONSTANT VS BIAS FIELD

EA17

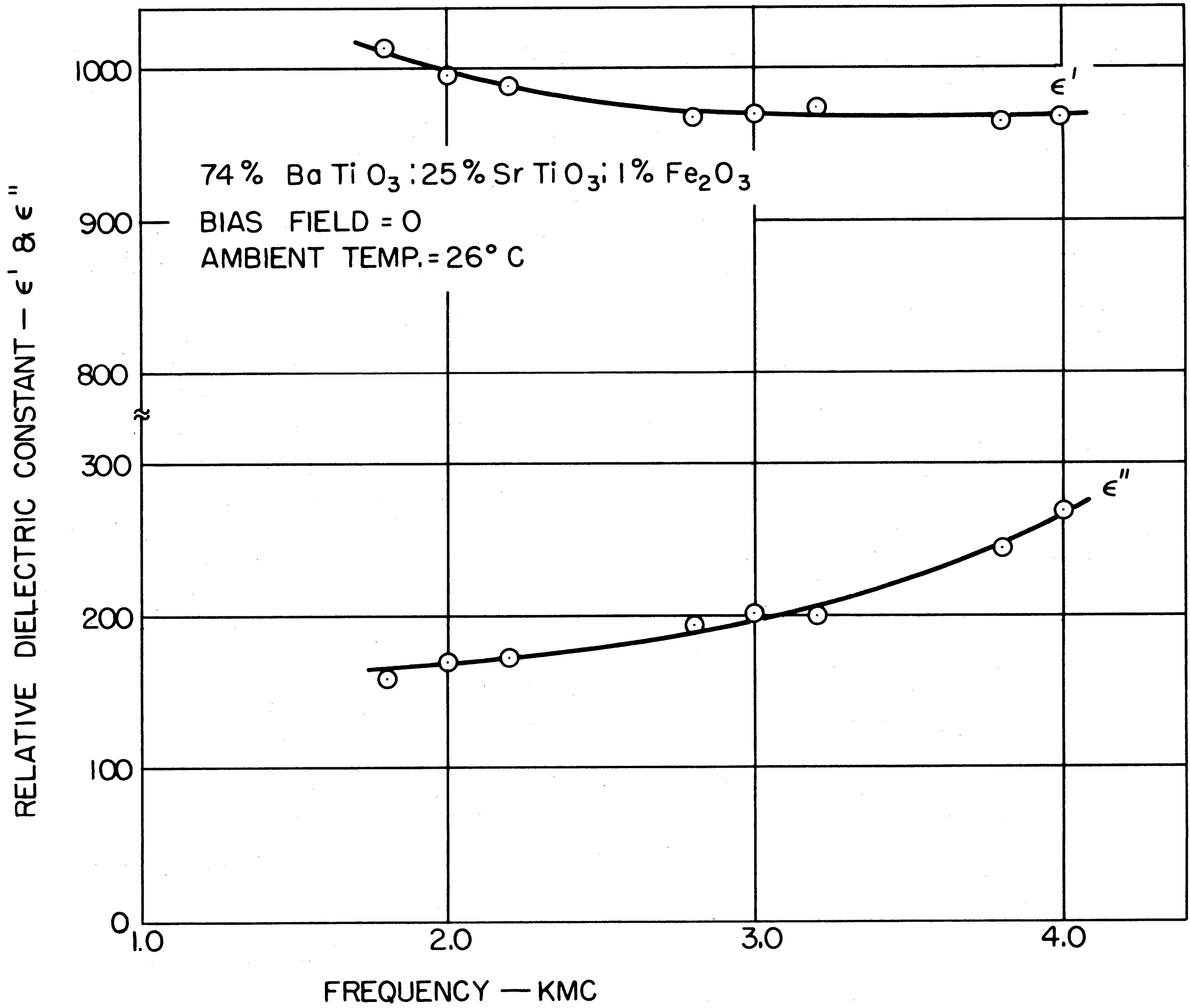

FIG.20 RELATIVE DIELECTRIC CONSTANT VS FREQUENCY

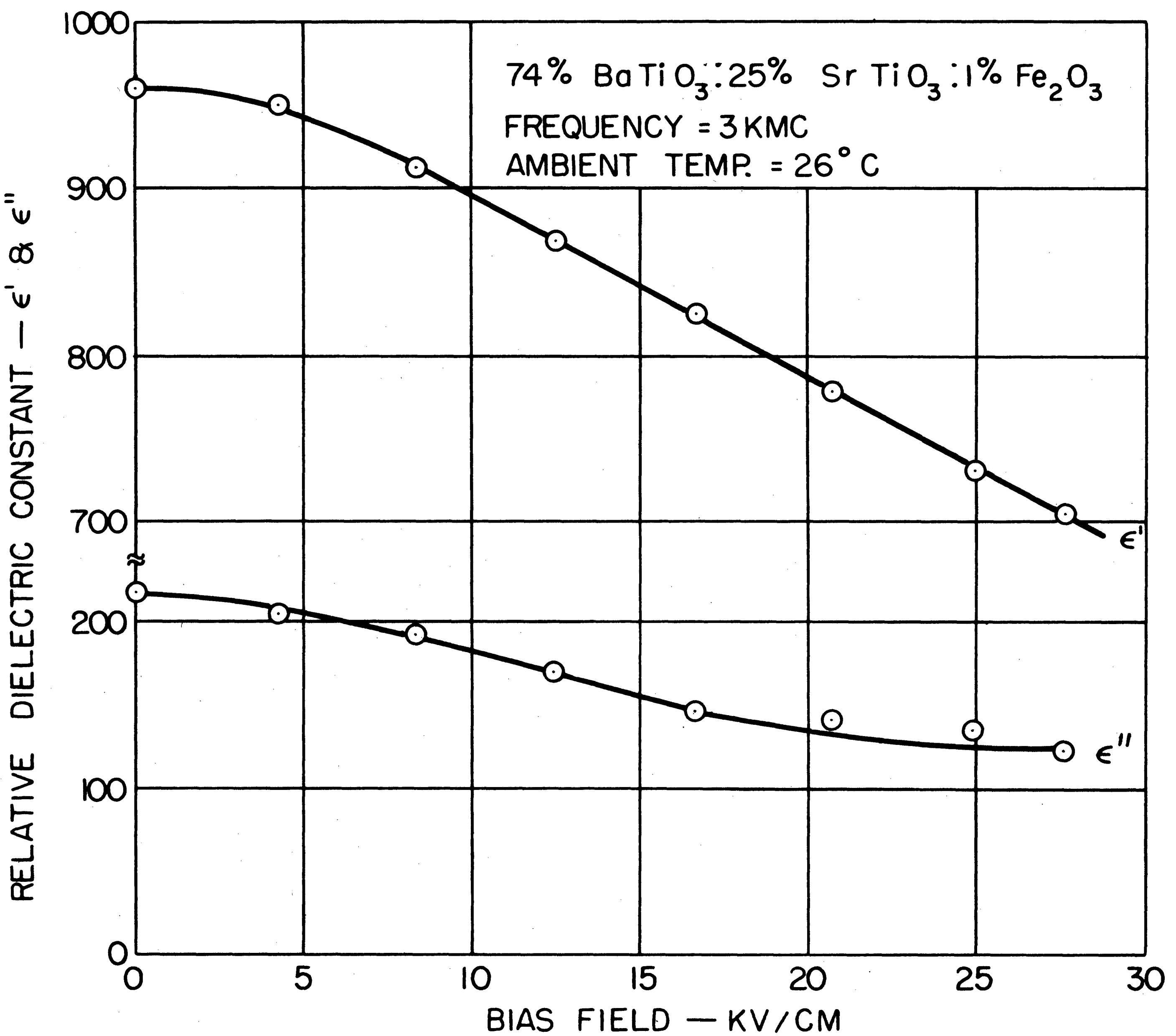

FIG. 21 RELATIVE DIELECTRIC CONSTANT VS BIAS FIELD

AD 49

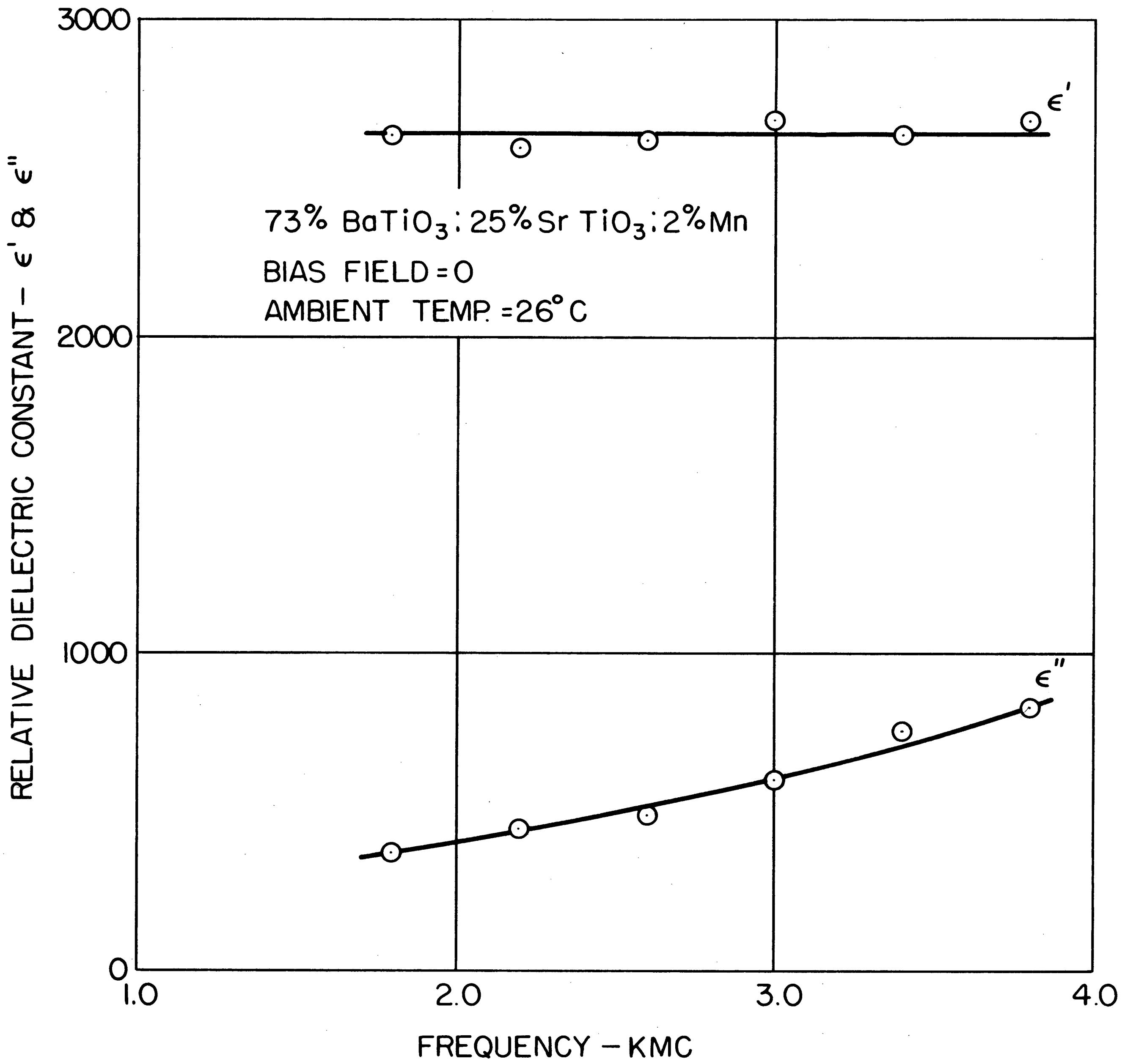

FIG.22 RELATIVE DIELECTRIC CONSTANT VS FREQUENCY

EA20

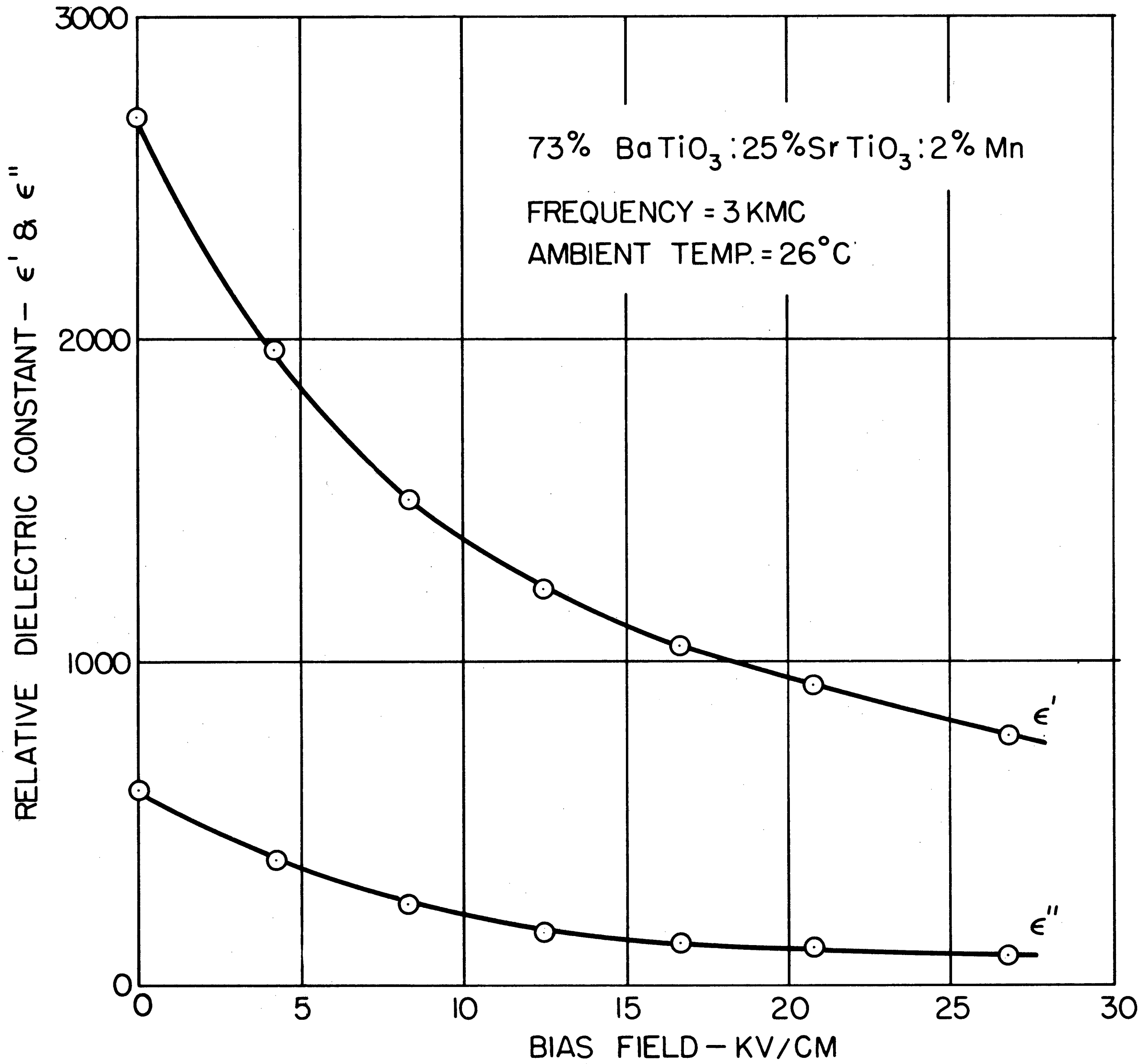

FIG. 23 RELATIVE DIELECTRIC CONSTANT VS BIAS FIELD

EA25

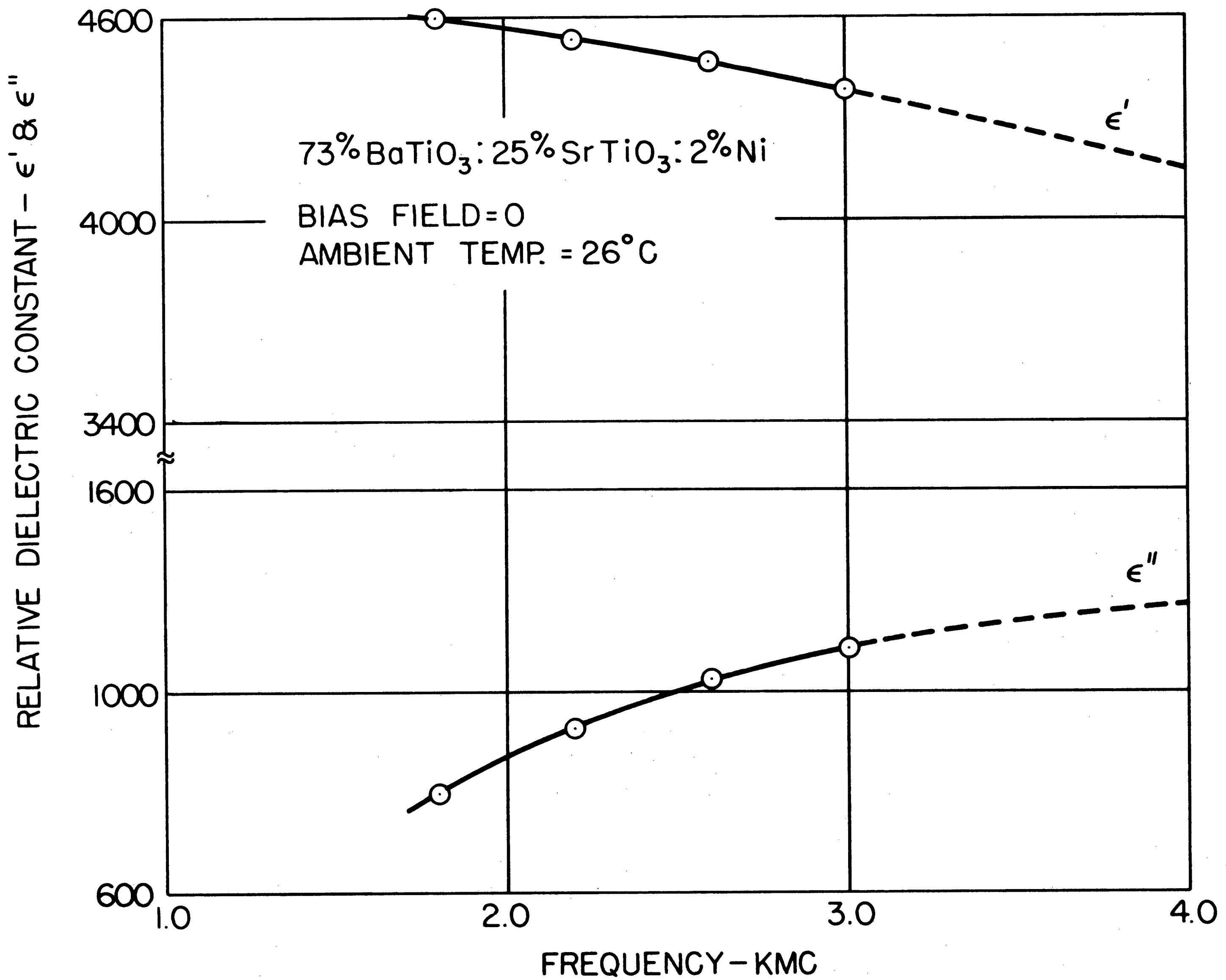

FIG. 24 RELATIVE DIELECTRIC CONSTANT VS FREQUENCY

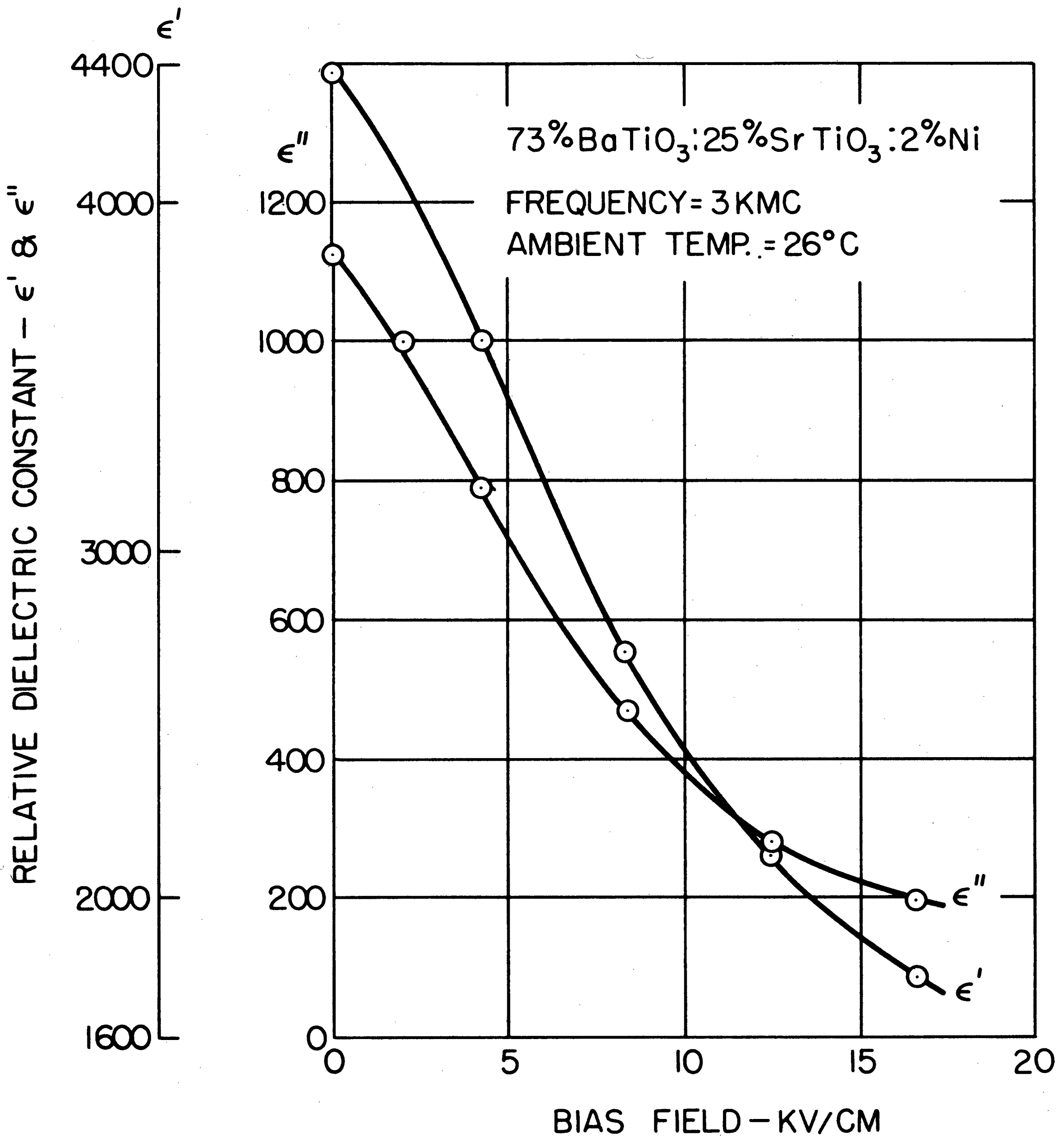

FIG. 25 RELATIVE DIELECTRIC CONSTANT VS BIAS FIELD

EA26

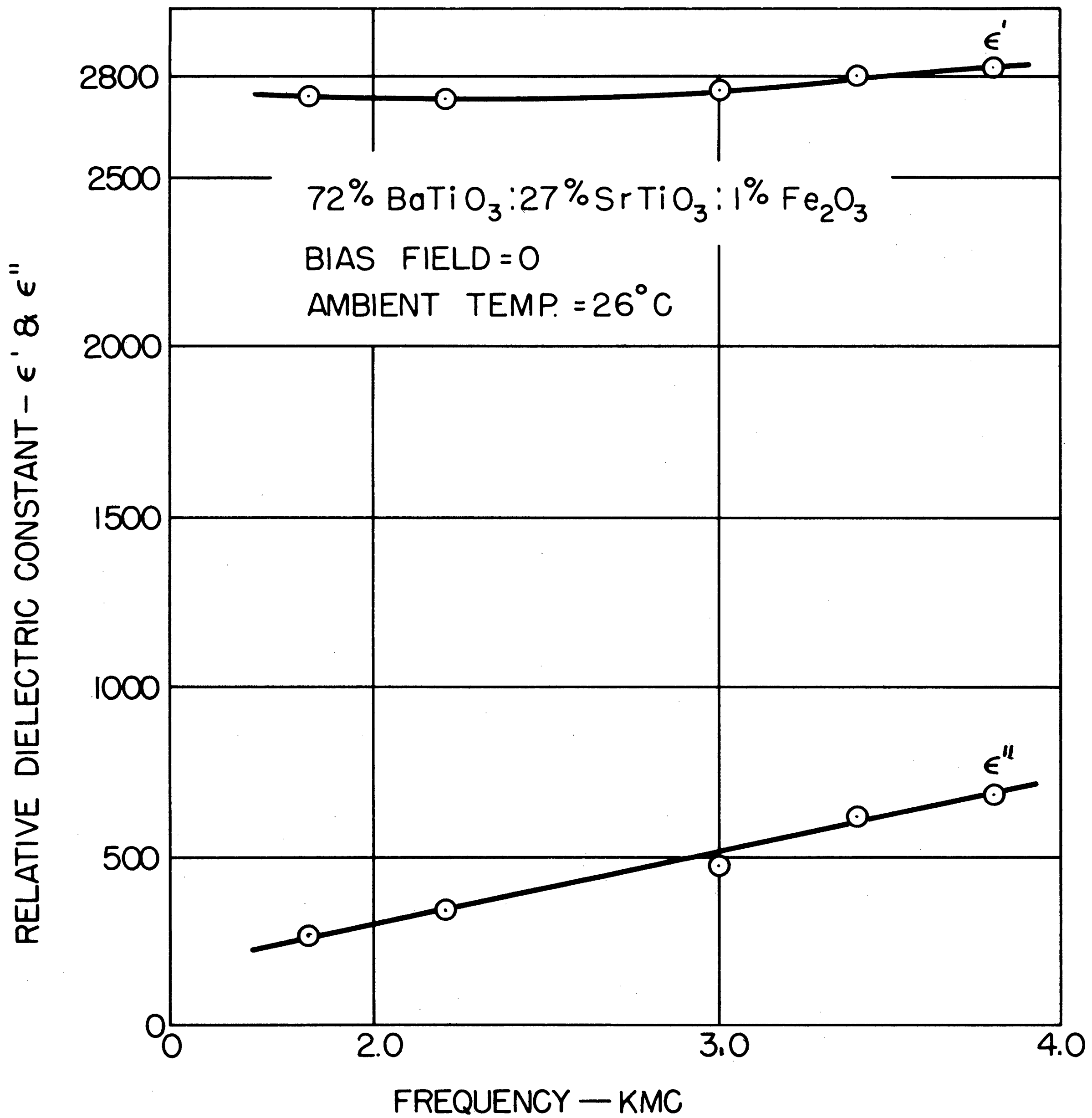

FIG.26 RELATIVE DIELECTRIC CONSTANT VS FREQUENCY

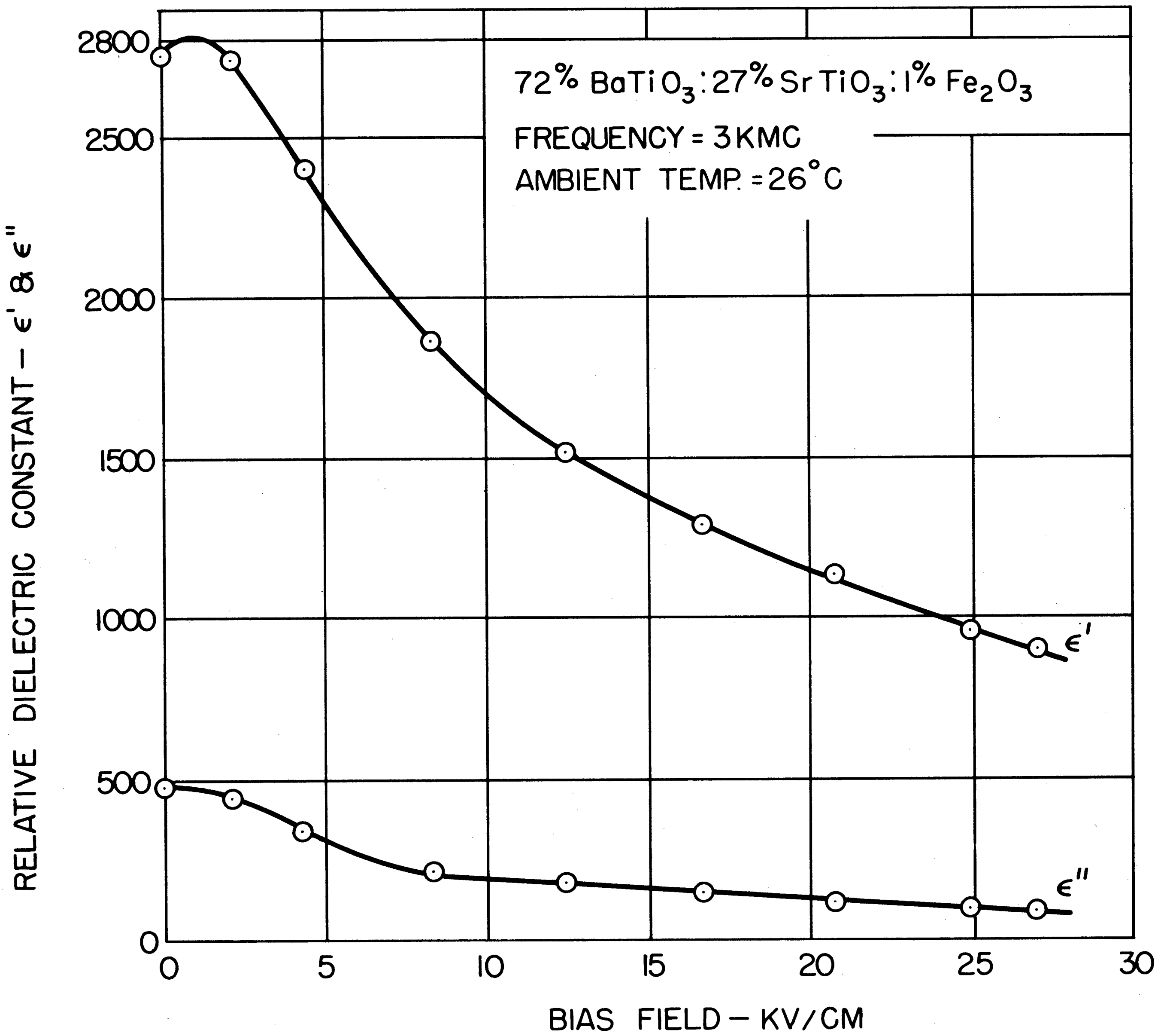

FIG.27 RELATIVE DIELECTRIC CONSTANT VS BIAS FIELD

EA28

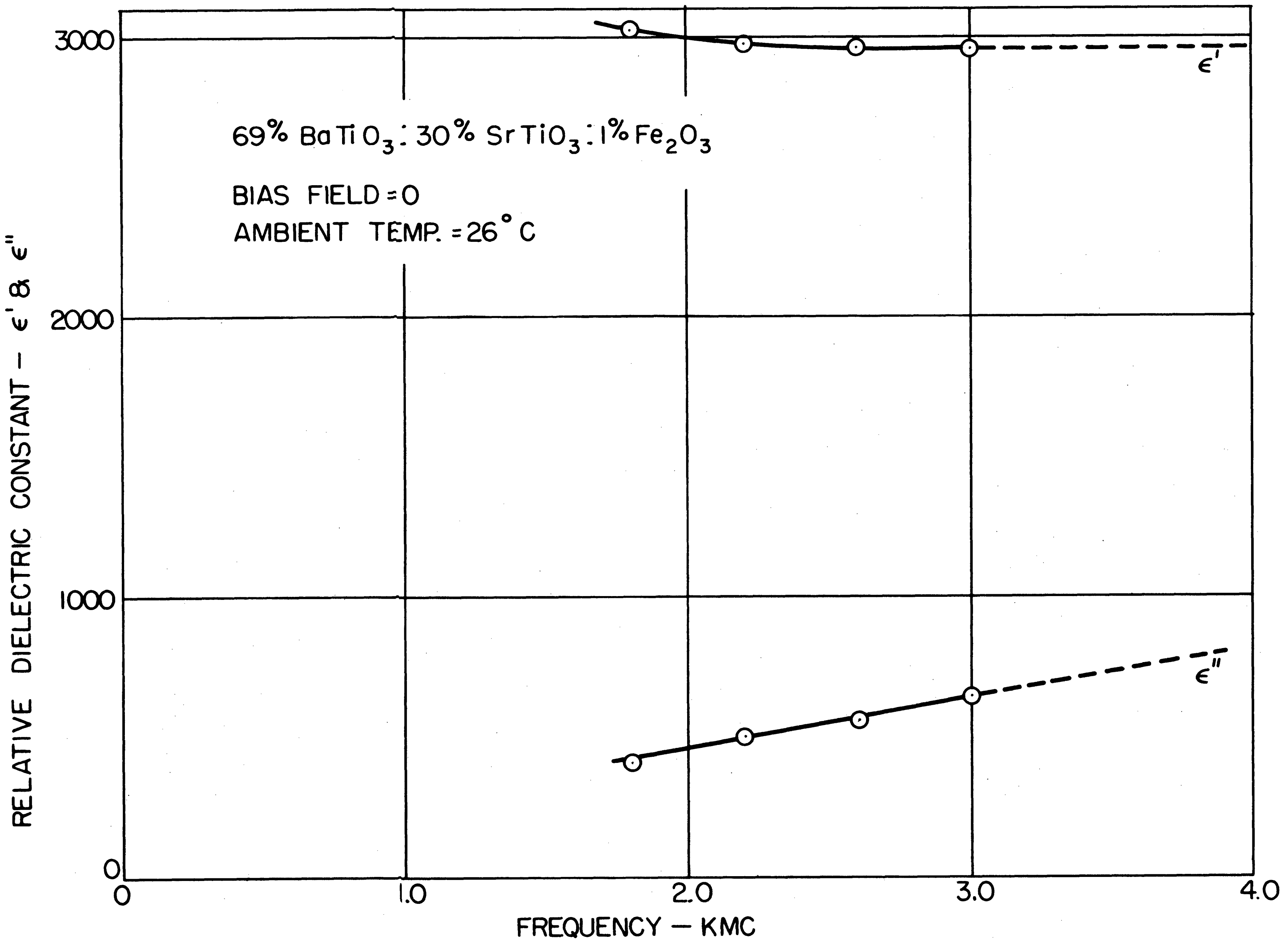

FIG. 28 RELATIVE DIELECTRIC CONSTANT VS. FREQUENCY

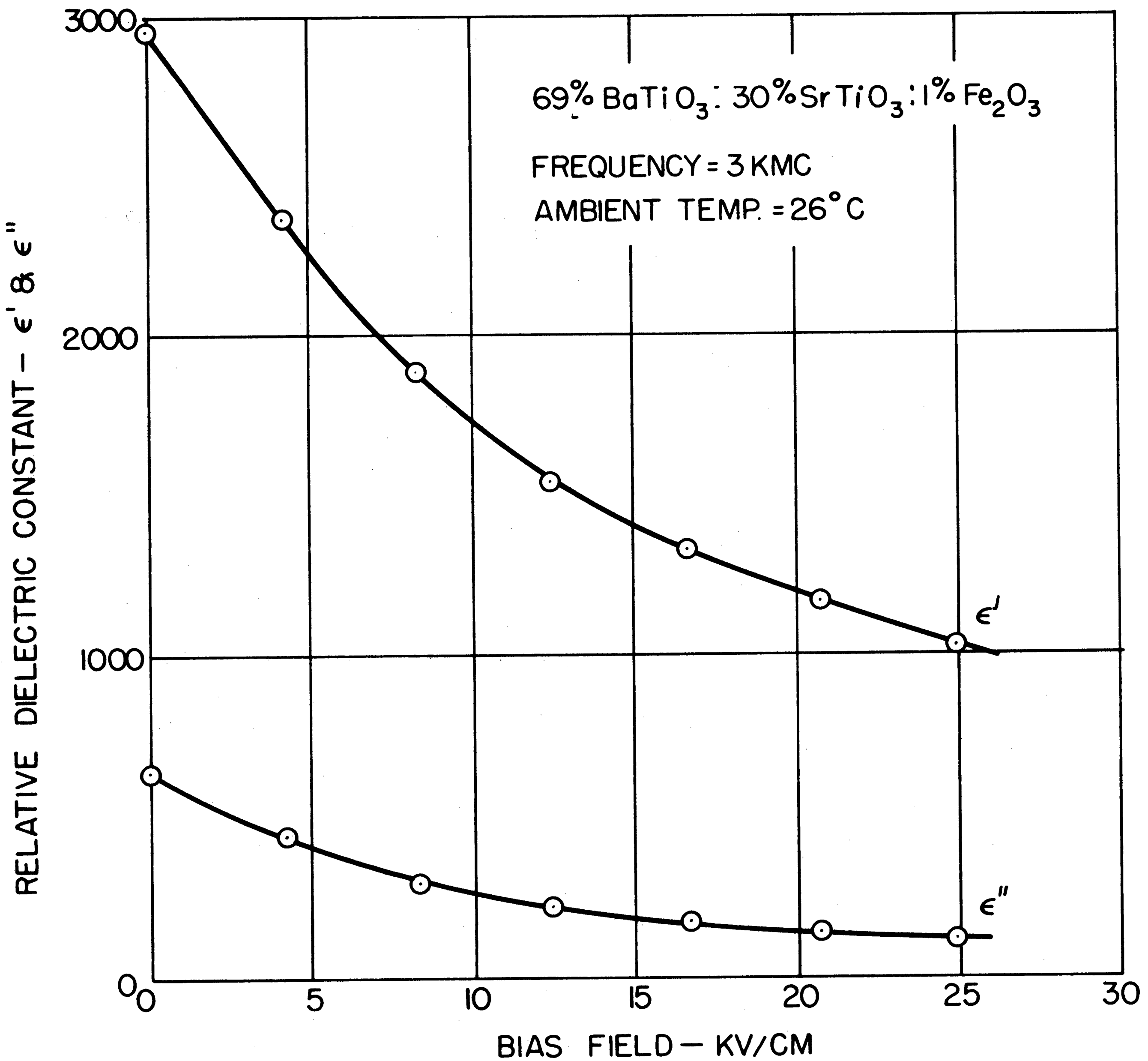

FIG. 29 RELATIVE DIELECTRIC CONSTANT VS BIAS FIELD

EA 24

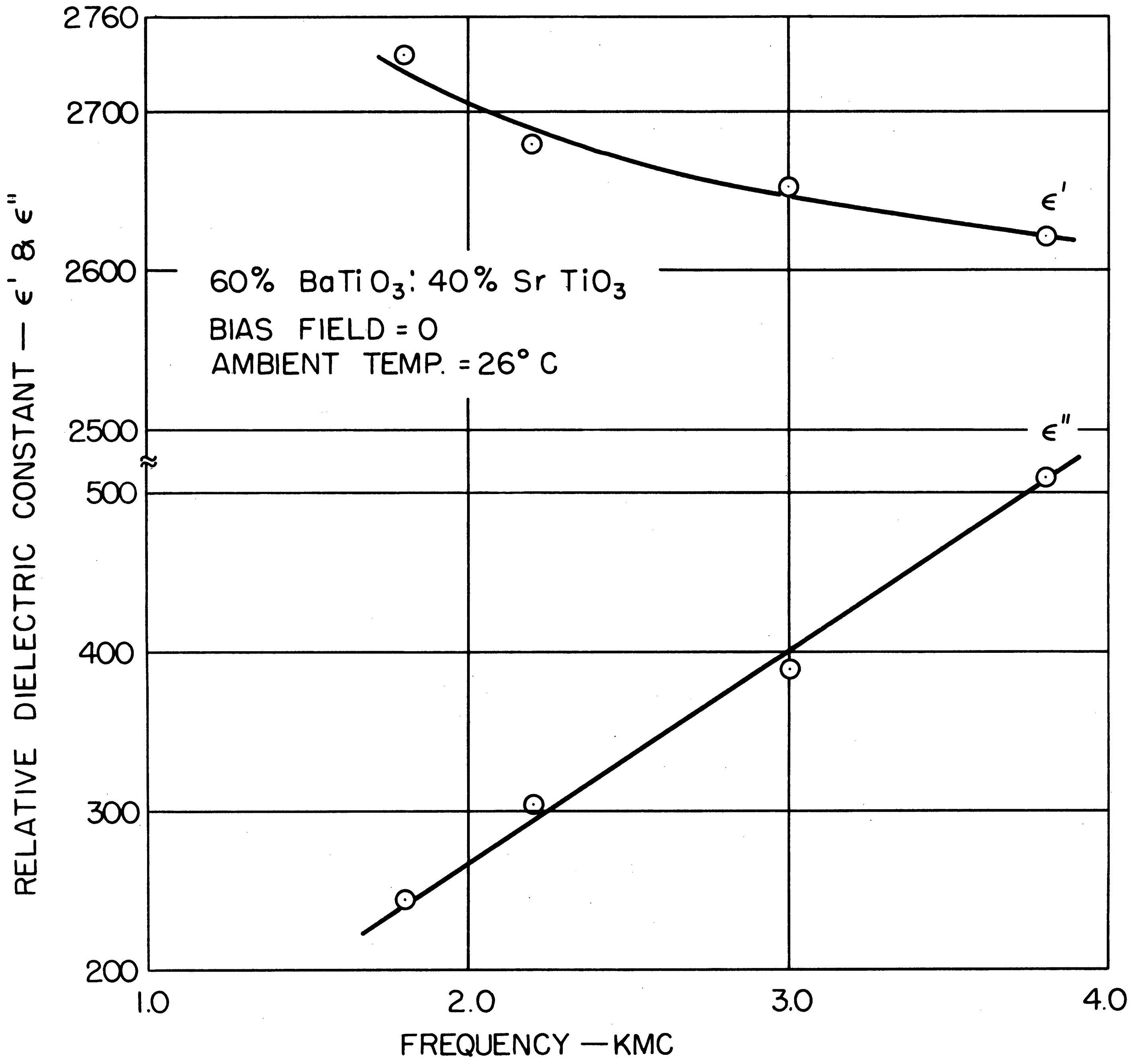

FIG. 30 RELATIVE DIELECTRIC CONSTANT VS FREQUENCY

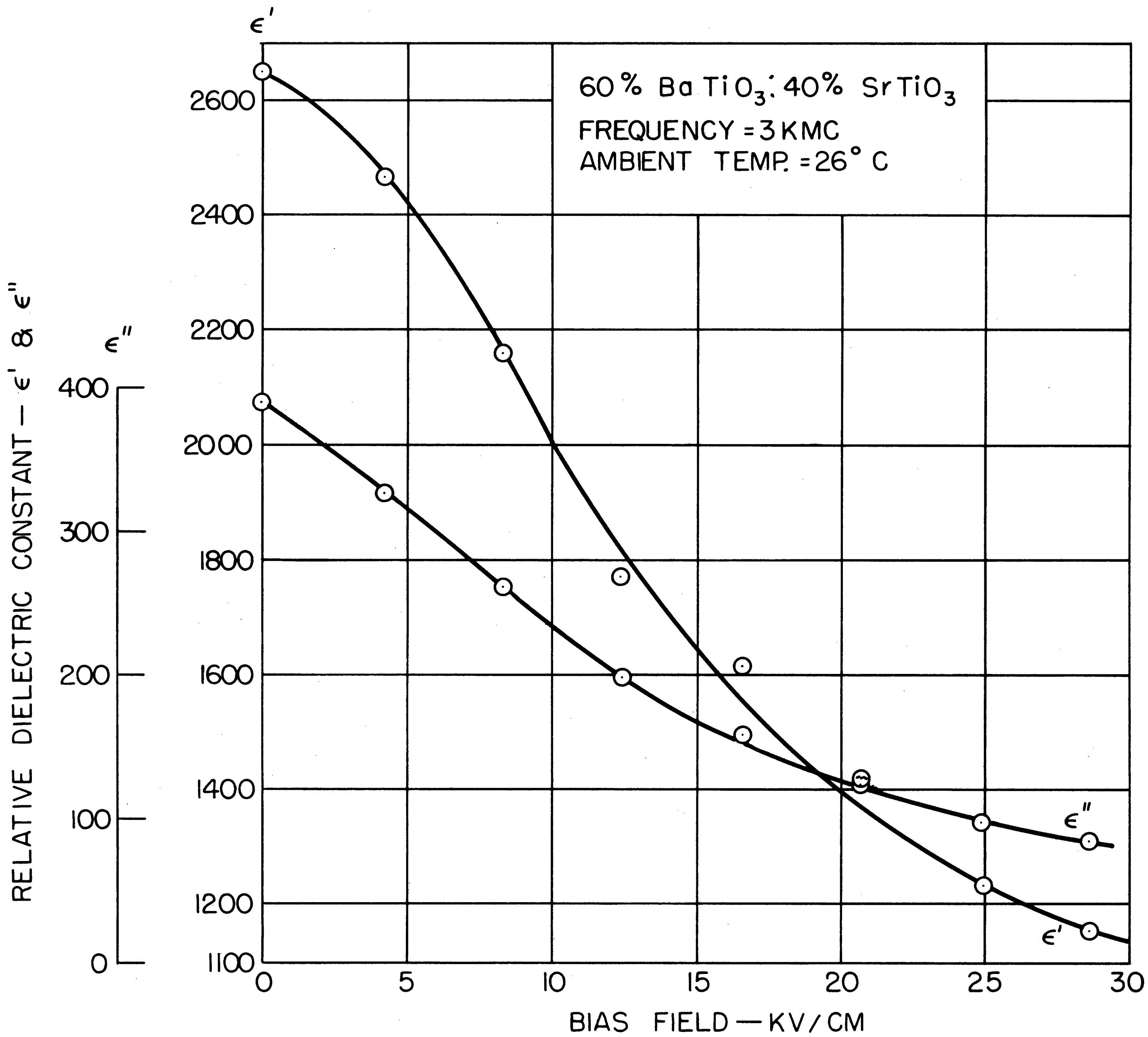

FIG. 31 RELATIVE DIELECTRIC CONSTANT VS BIAS FIELD

DA 50

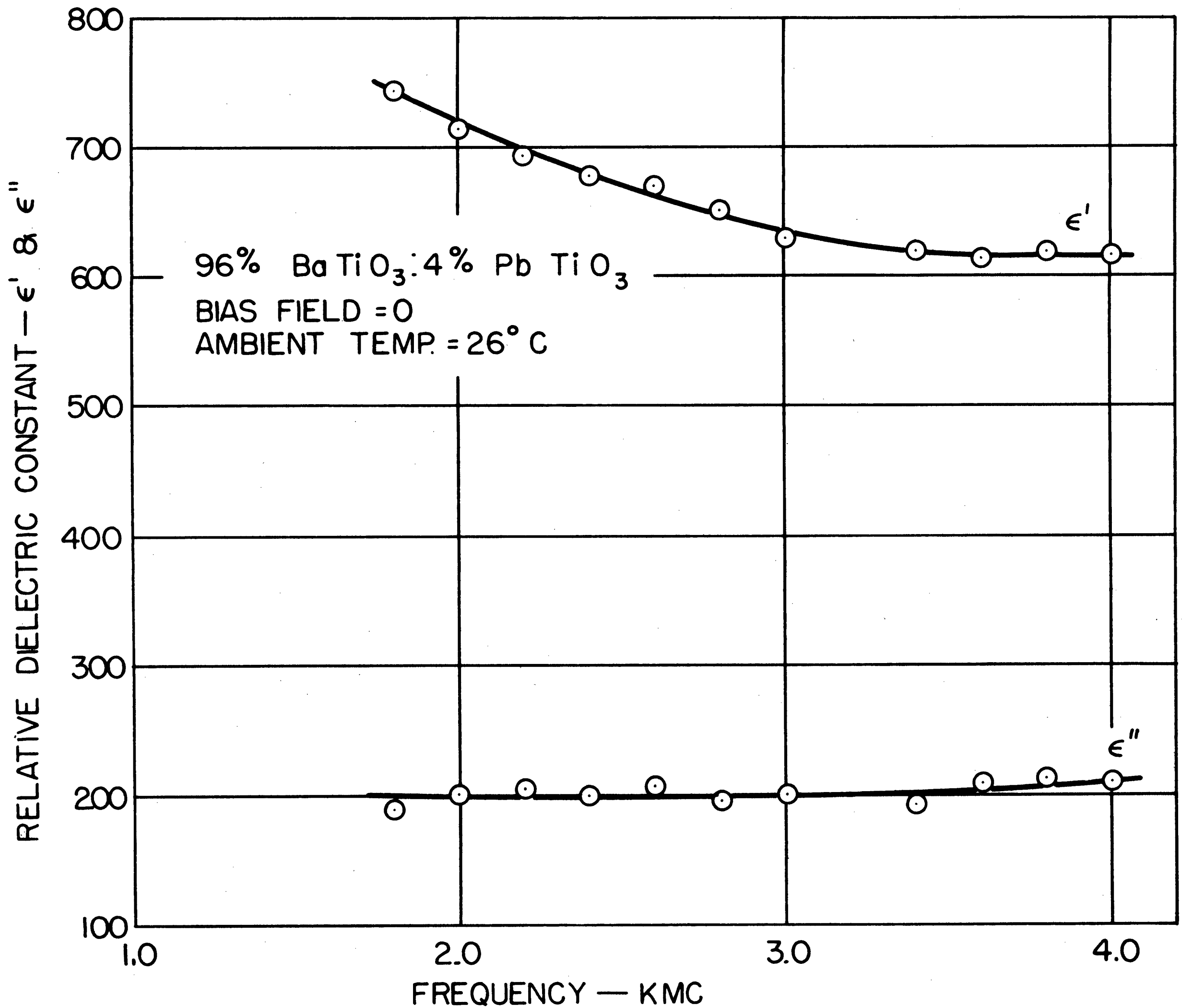

FIG.32 RELATIVE DIELECTRIC CONSTANT VS FREQUENCY

EA 8

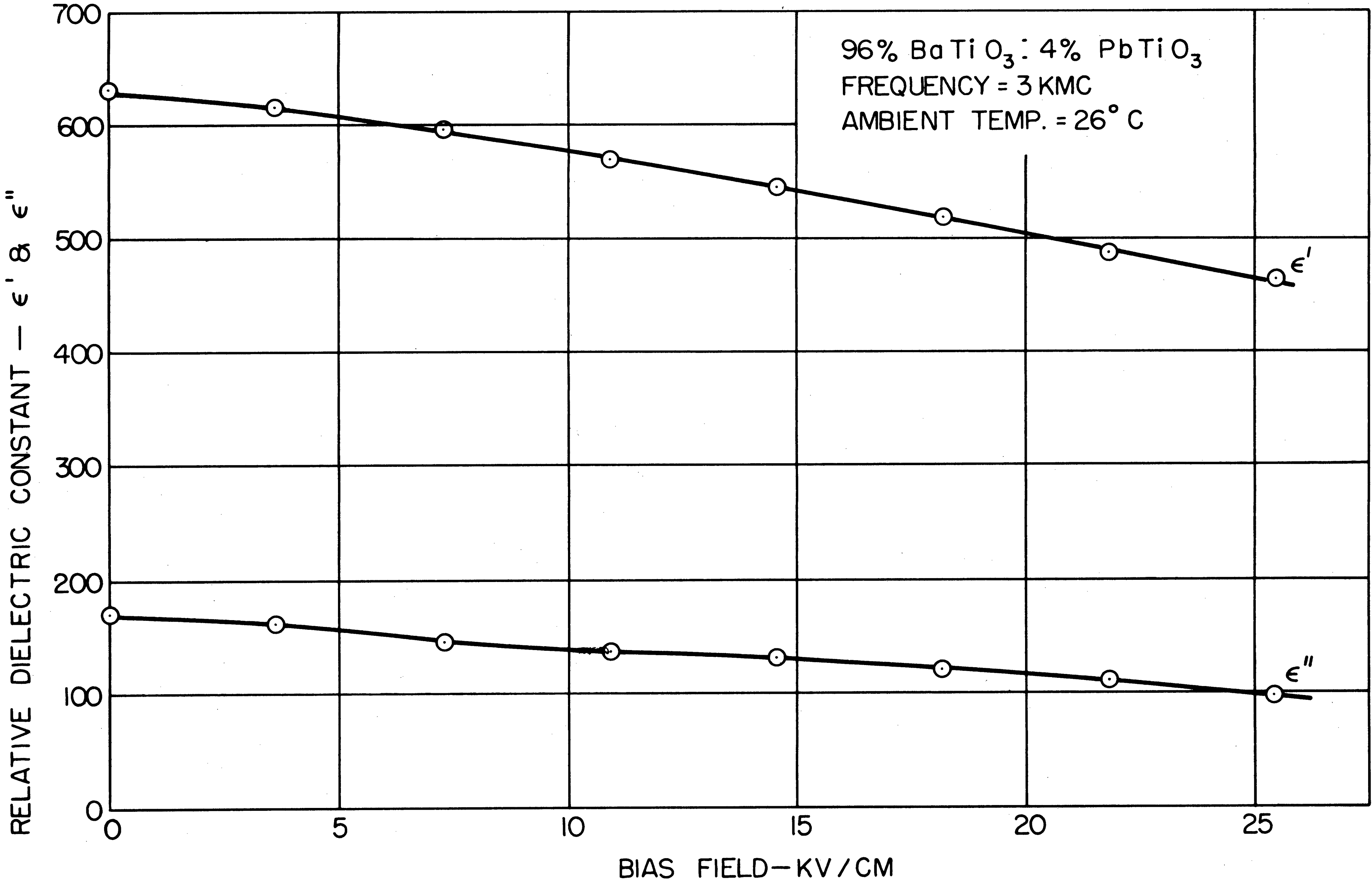

FIG. 33 RELATIVE DIELECTRIC CONSTANT VS BIAS FIELD

AD48

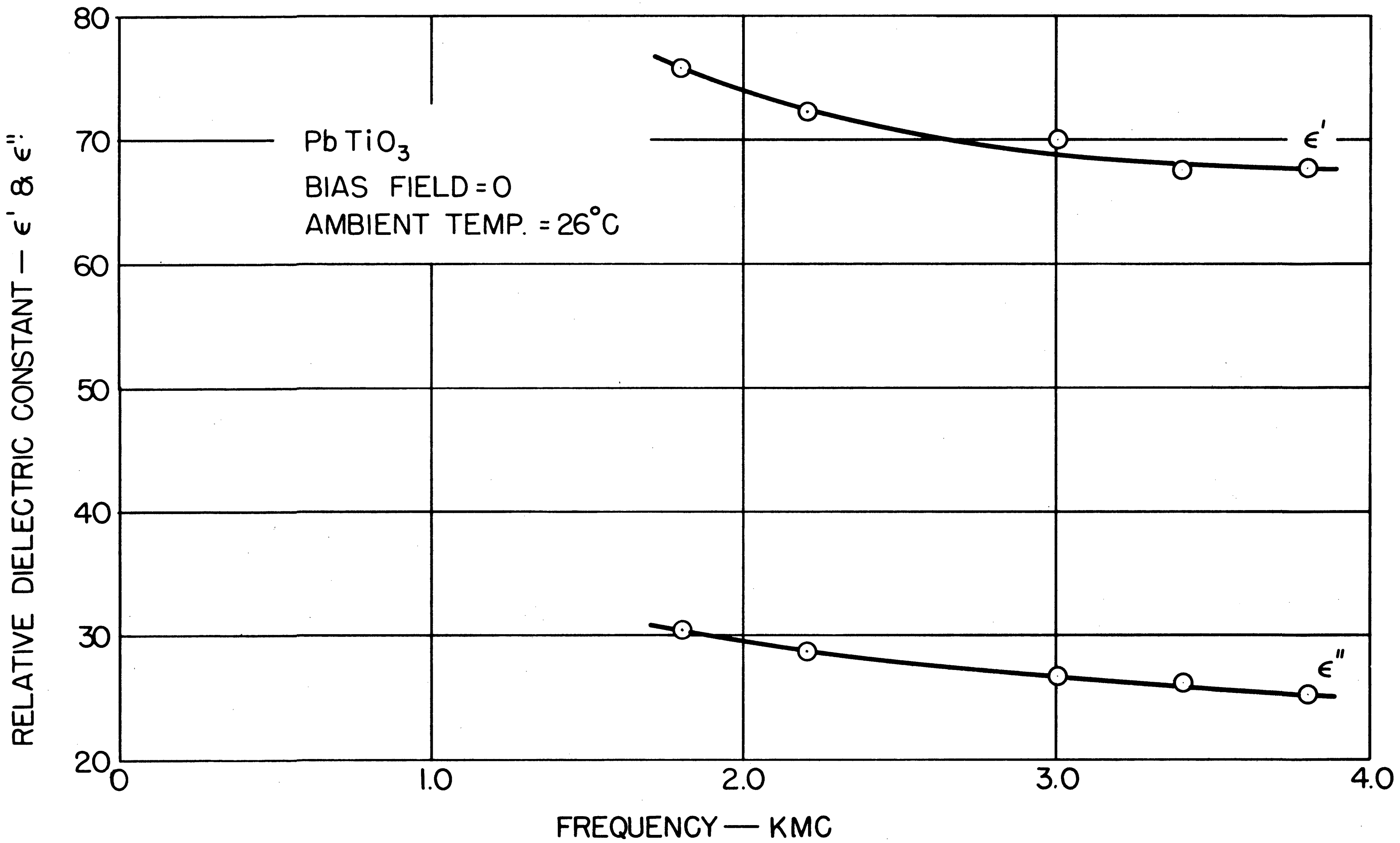

FIG. 34 RELATIVE DIELECTRIC CONSTANT VS FREQUENCY

EA35

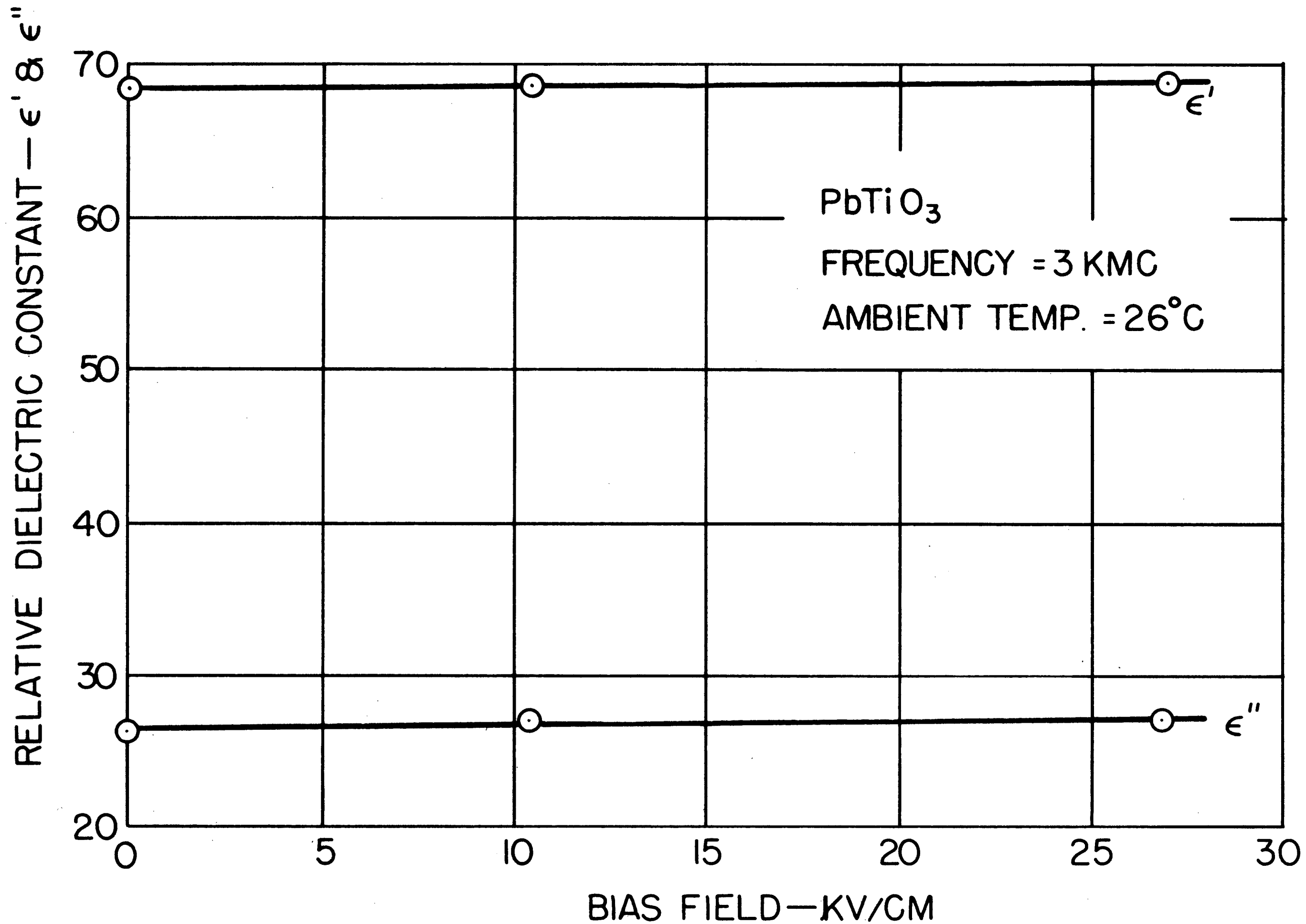

FIG. 35 RELATIVE DIELECTRIC CONSTANT VS BIAS FIELD

EA 28

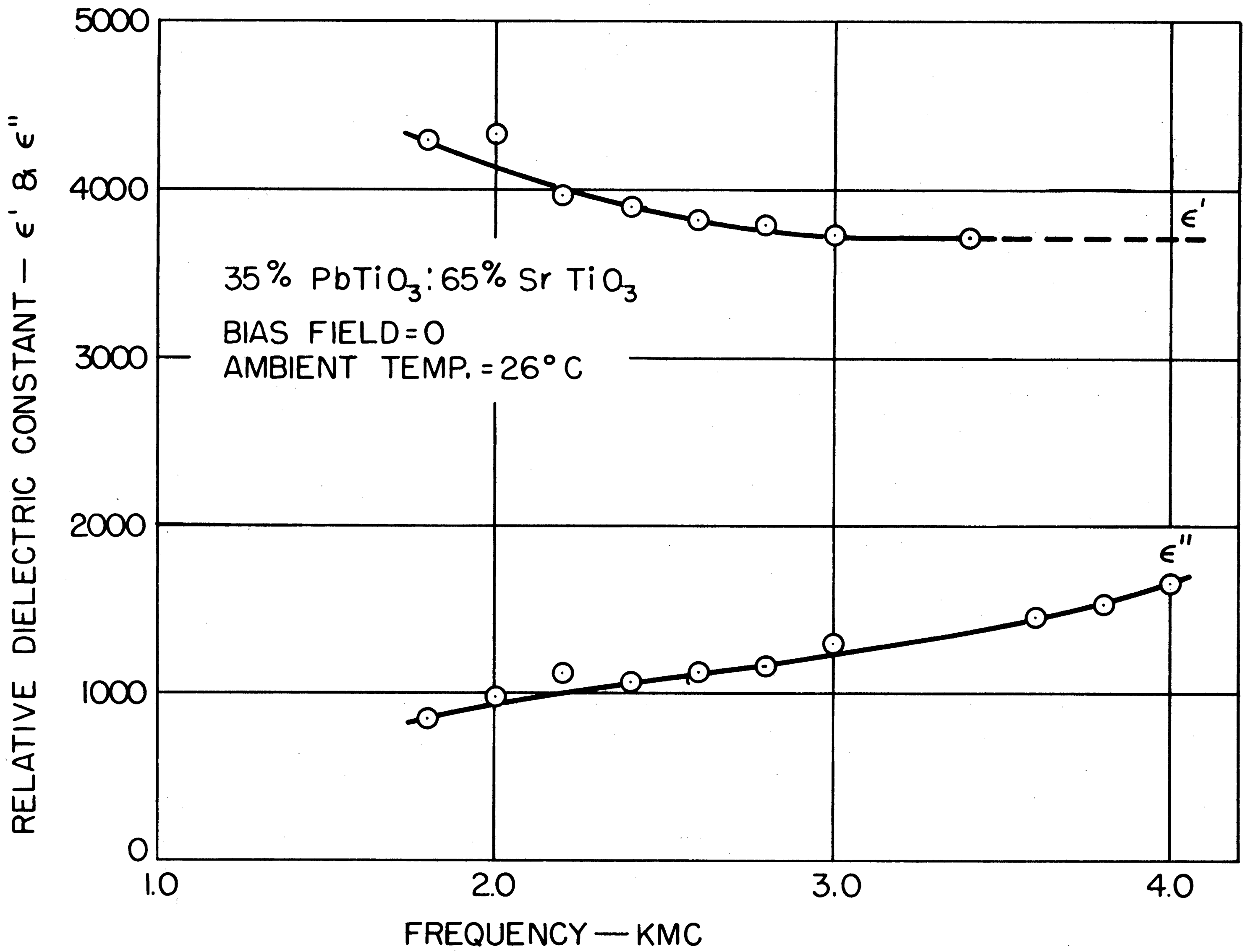

FIG. 36 RELATIVE DIELECTRIC CONSTANT VS FREQUENCY

EA11

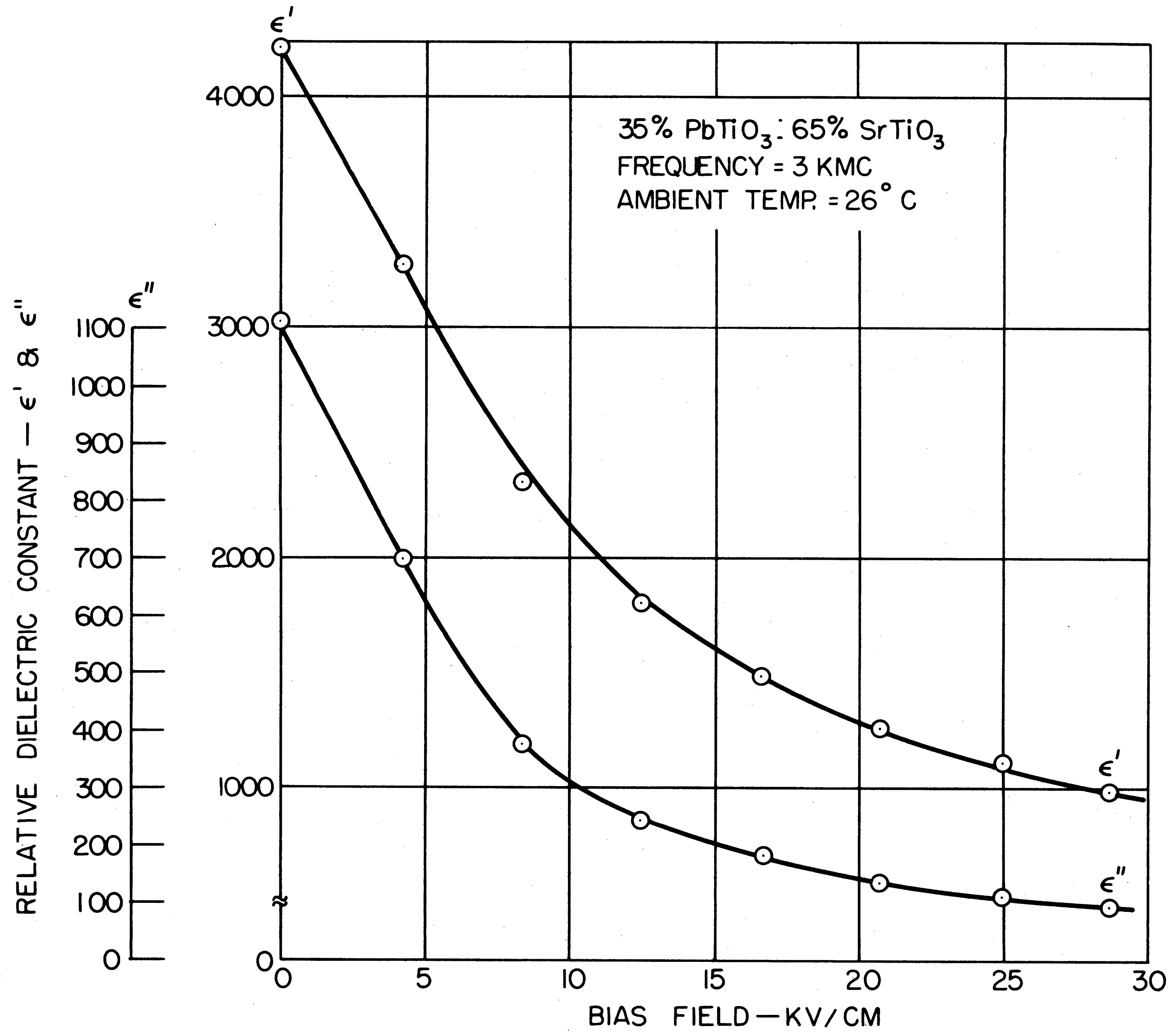

FIG. 37 RELATIVE DIELECTRIC CONSTANT VS BIAS FIELD

AD 46

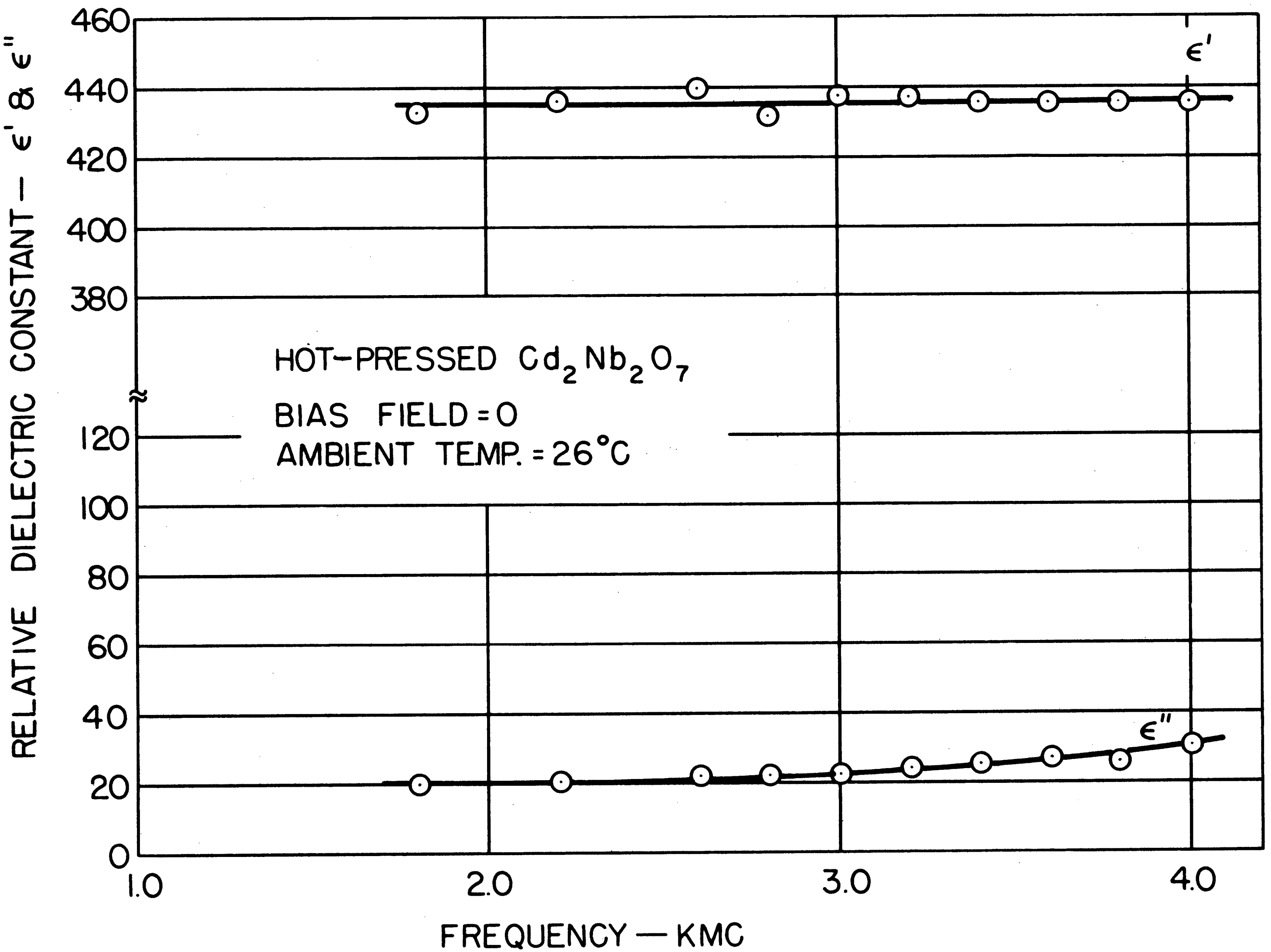

FIG. 38 RELATIVE DIELECTRIC CONSTANT VS FREQUENCY

FA23

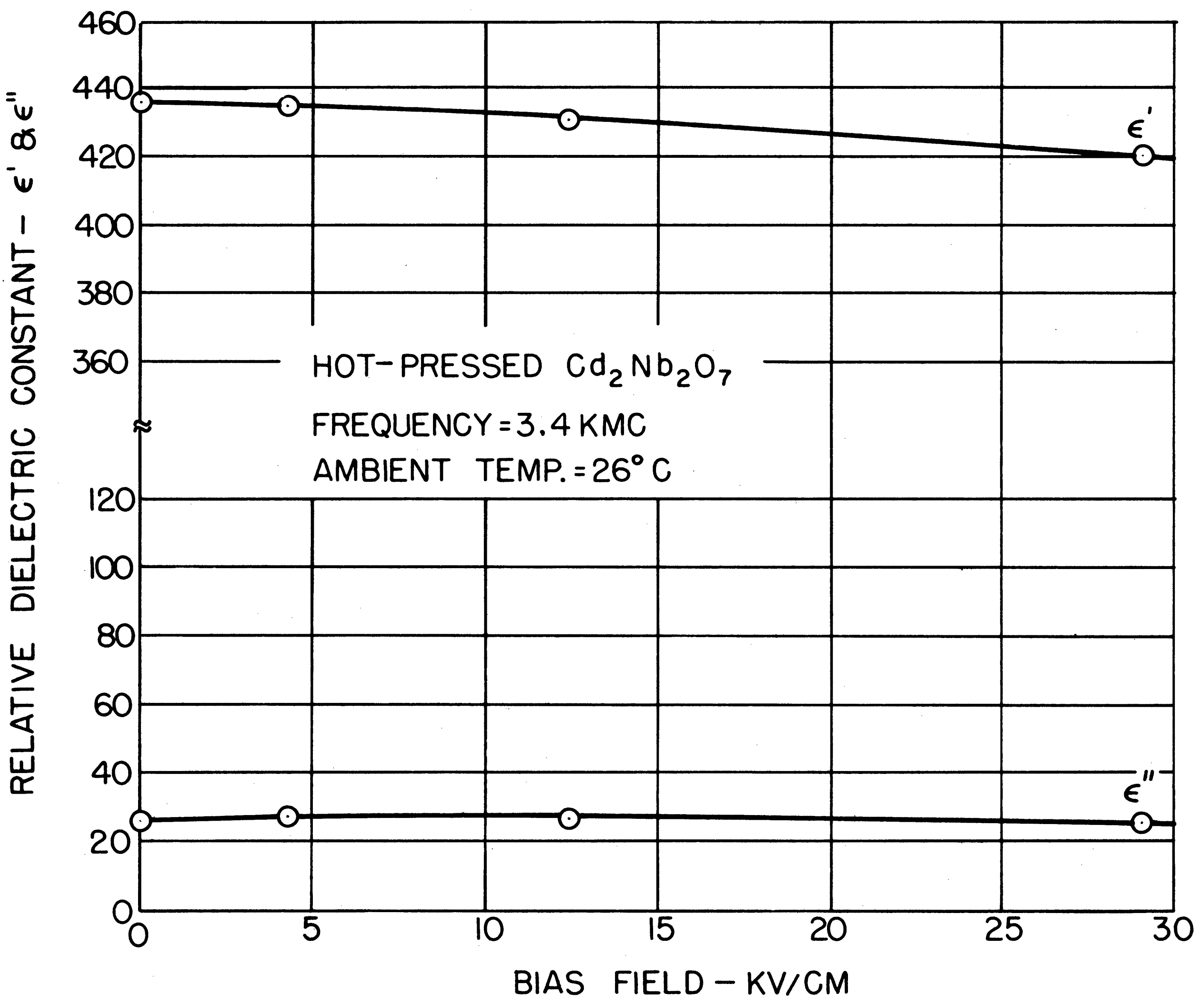

FIG.39 RELATIVE DIELECTRIC CONSTANT VS BIAS FIELD

EA27

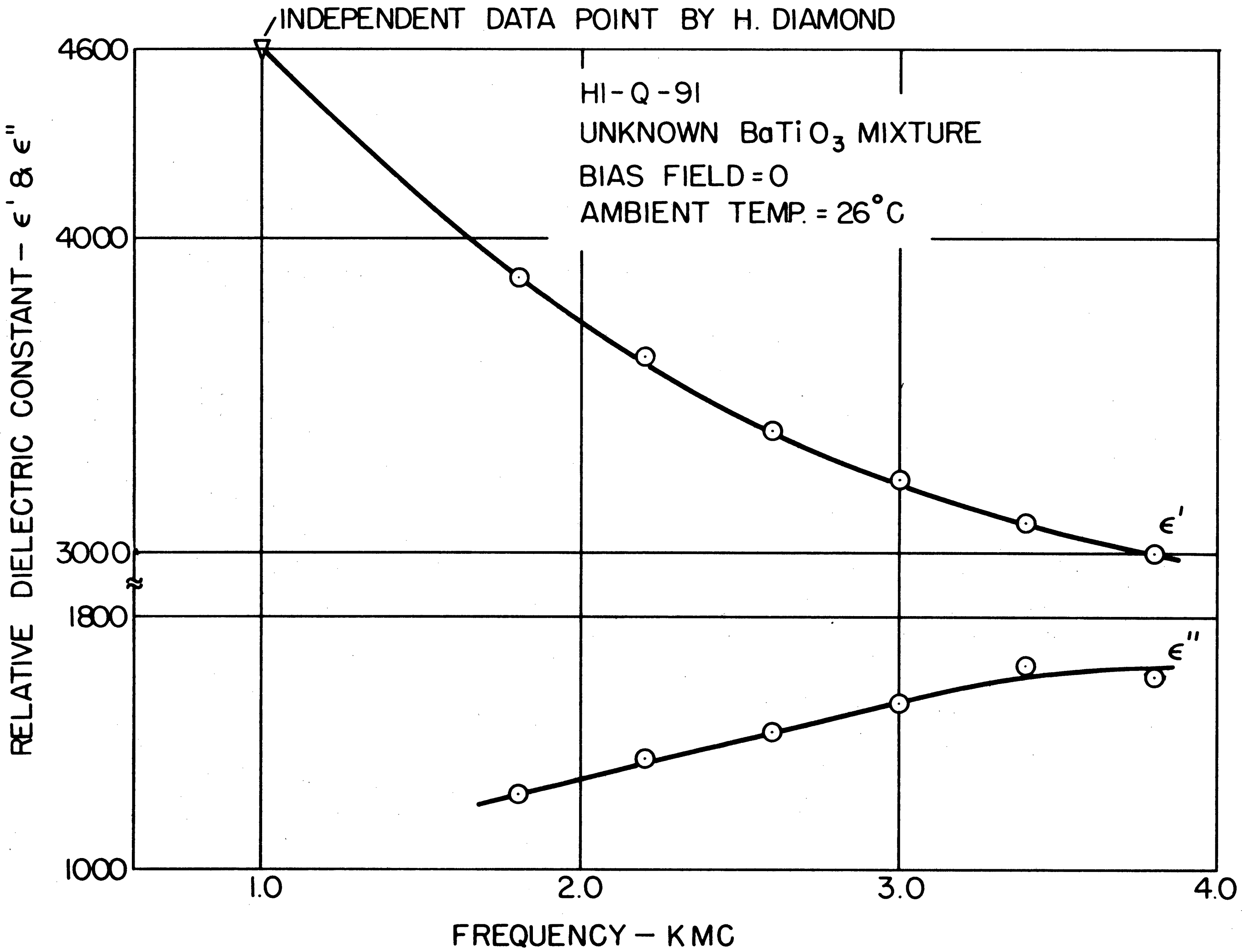

FIG. 40 RELATIVE DIELECTRIC CONSTANT VS FREQUENCY

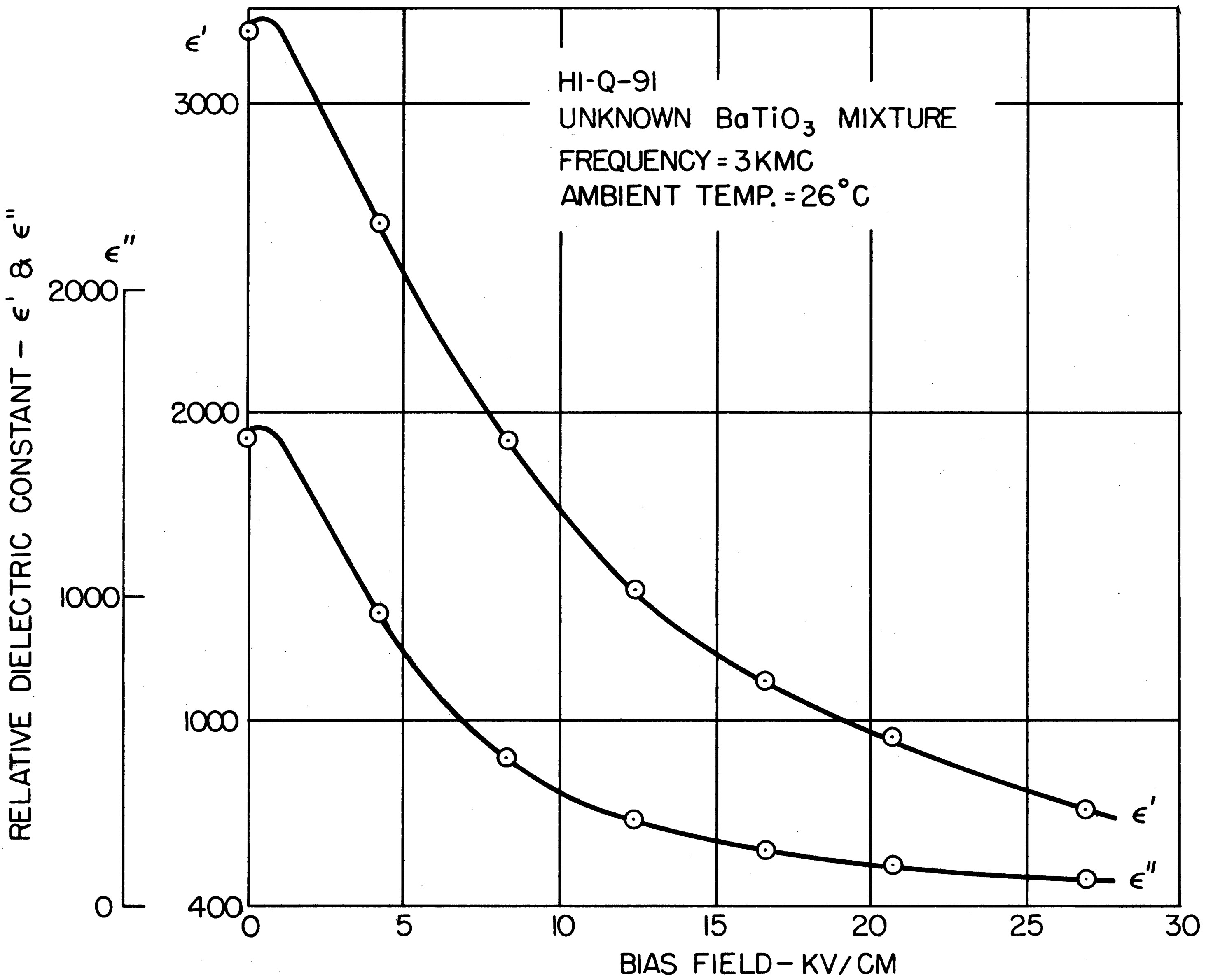

FIG.41 RELATIVE DIELECTRIC CONSTANT VS BIAS FIELD

EA 31

REFERENCES

1. Powles and Jackson, Proc. Inst. Elec. Engrs., Part III, 96, 383, 1949.
2. A. von Hippel, Rev. Mod. Phys., 22, 221, 1950.
3. Davis and Rubin, J. Appl. Phys., 24, 1194, 1953.
4. C. Kittel, Introduction to Modern Physics, John Wiley and Sons, Inc., New York, 1956, p. 202.
5. Oliner and Altschuler, J. Appl. Phys., 26, 214, 1953.
6. A. von Hippel, Dielectric Materials and Applications, John Wiley and Sons, Inc., New York, 1954, p. 69.
7. N. Marcuvitz, Waveguide Handbook, Rad. Lab. Series, Vol. 10, McGraw-Hill, New York, 1951, p. 119.
8. ibid., p. 33.
9. Whittaker and Watson, Modern Analysis, MacMillan, London, 1946, p. 380.
10. Willis and Sinha, J. Inst. Elec. Engrs., Part VIIB, 103, 166, 1956.
11. W. M. Nunn, Jr. "Standing Wave Measurements in Coaxial Systems," Electronic Defense Group Technical Report No. 87, The University of Michigan, Ann Arbor, Michigan, 1958.
12. A. M. Winzemer, Proc. IRE, 38, 275, 1950.
13. Powles and Jackson, op.cit.

DISTRIBUTION LIST

1 Copy	Technical Document Services Bldg. 255 Willow Run Laboratories The University of Michigan Ypsilanti, Michigan
1 Copy	The University of Michigan Research Institute Project File Ann Arbor, Michigan
10 Copies	Electronic Defense Group Project File The University of Michigan Research Institute Ann Arbor, Michigan
50 Copies	Activity Supply Officer, USASRDL Building No. 2504 Watson Area Fort Monmouth, New Jersey FOR: ELECTRON DEVICES DIVISION Inspect at Destination File No. 0130-PH-58-91(1563)

ps

UNIVERSITY OF MICHIGAN
3 9015 03524 4063